Clay Minerals, (2016) **51**, 539–562

Geological features and geochemical characteristics of Late Devonian–Early Carboniferous K-bentonites from northwestern Turkey

M.C. GÖNCÜOĞLU[1,†], A. GÜNAL-TÜRKMENOĞLU[1], Ö. BOZKAYA[2,*], Ö. ÜNLÜCE-YÜCEL[1], C. OKUYUCU[3] AND İ.Ö. YILMAZ[1]

[1] *Department of Geological Engineering, Middle East Technical University, Ankara, Turkey*
[2] *Department of Geological Engineering, Pamukkale University, Denizli, Turkey*
[3] *Department of Geological Engineering, Selçuk University, Konya, Turkey*

(*Received 6 December 2015; revised 14 June 2016; Editor: George Christidis*)

ABSTRACT: Newly discovered K-bentonite beds, interstratified with limestones/dolomitic limestones of the Upper Devonian–Lower Carboniferous Yılanlı Formation, are exposed in the northwestern Black Sea region of Turkey, around Zonguldak and Bartın. K-bentonite samples collected from four different locations: the Gavurpınarı and Yılanlı Burnu quarries from the Bartın area, the Çimşir Çukurları quarry from the Şapça area, and the Güdüllü and Gökgöl highway tunnel section near Zonguldak city were investigated using optical microscopy, X-ray diffraction and inductively coupled plasma mass spectrometry in order to reveal their mineralogical and geochemical characteristics and understand their origin and evolution. The K-bentonites occur at different levels in the Yılanlı Formation as 2–40 cm-thick, greenish to yellowish beds cropping out several hundred metres along strike. Preliminary biostratigraphic data suggest that the protoliths of the Bartın (Gavurpınarı and Yılanlı Burnu) and Güdüllü K-bentonites were deposited at around the boundary between the Frasnian and Famennian, whereas those in the Şapça and Gökgöl sections are slightly younger (Devonian–Carboniferous boundary interval). The lithofacies types of the host carbonate rocks suggest an 'epeiric' shallow carbonate platform environment. Illite and mixed-layer illite-smectite were the major clay minerals in the K-bentonites. The K-bentonites from the Bartın area display a high degree of illitization and consist mainly of illite indicating high-grade diagenesis, whereas illite-smectite-rich samples from the Şapca and Gökgöl tunnel locations reflect relatively lower diagenetic conditions. According to their geochemical compositions, two groups of K-bentonites were distinguished, one with alkali basalt (Bartın area and Güdüllü locations) and one with trachyte affinities (Gökgöl tunnel and Şapça locations). Geochemical fingerprinting of K-bentonites by trace and rare earth element (*REE*) data suggest that tephras with alkali basalt composition have been derived by a source formed in a 'continental back-arc' setting, whereas the source of K-bentonites with trachytic precursors is related to 'continental within-plate rifting'. An evaluation of the global Late Devonian and Devonian–Carboniferous volcanism suggests that the bentonite precursors may be related to late-Variscan magmatism in Laurussia.

KEYWORDS: K-bentonite, Late Devonian–Early Carboniferous, chemostratigraphy, tectonomagmatic setting, illite, Yilanli Formation, Turkey.

* E-mail: obozkaya@pau.edu.tr
[†]This work was originally presented during the session 'Bentonites linking clay science with technology', part of the Euroclay 2015 conference held in July 2015 in Edinburgh, UK.
DOI: 10.1180/claymin.2016.051.4.02

The products of explosive eruptions in the form of volcanic ash (tephra), after transport over long distances, are settled and altered to bentonites (smectite-rich volcanogenic clay rocks) by early

diagenesis. During late diagenesis, these bentonites are transformed into K-bentonites by chemical modification and progressive illitization, and then finally into metabentonites by low-grade metamorphism (Fortey *et al.*, 1996). During diagenesis and very low-grade metamorphism, smectite transforms to mixed-layer illite-smectite and then to illite in K-bentonites, due to K enrichment (Weaver, 1953; Merriman & Roberts, 1990). K-bentonites are accepted as useful time markers of geologically instantaneous chronostratigraphic surfaces due to their sudden eruption, rapid accumulation rate and widespread distribution. Thus, they have large potential for local and regional palaeogeographical, sedimentological, biogeographical and palaeoecological correlations (Huff & Morgan, 1990; Kolata *et al.*, 1998; Min *et al.*, 2001). Another aspect of interest is their relationship with mass extinctions (Algeo *et al.*, 1995).

The geochemistry of K-bentonites provides significant data for the tectonomagmatic evolution of the source area, and also for the former positions of continental plates through the distribution patterns of ash beds which are a significant distance apart (Kolata *et al.*, 1987; Huff *et al.*, 1992; Bergström *et al.*, 1995). Previous investigations showed that interpretation of the tectonic setting and genesis of K-bentonites may be achieved by magmatic and tectonic discrimination diagrams (Winchester & Floyd, 1977; Floyd & Winchester, 1978; Huff & Türkmenoğlu, 1981; Merriman & Roberts, 1990; Huff *et al.*, 1992).

Although extensive research has been performed worldwide on K-bentonites of volcanic origin, their first discovery in Turkey was published recently (Türkmenoğlu, 2001; Türkmenoğlu *et al.*, 2009; Günal-Türkmenoğlu *et al.*, 2015). In the Zonguldak Terrane (ZT) in NW Turkey (Fig. 1a,b), K-bentonites are exposed in the Upper Devonian–Lower Carboniferous strata (Yılanlı Formation) in the Zonguldak and Bartın areas (Fig. 1c,d). They form a set of 2–40 cm-thick greenish-grey clay beds alternating with platform-type, shallow-marine limestones and dolomitic limestones of the Yılanlı Formation.

Ongoing research into Turkish K-bentonites has resulted in the discovery of new locations within the Gökgöl Tunnel, in the Şapça and Güdüllü areas to the south of Zonguldak (Fig. 1c), and in similarly well preserved sequences within the limestones and dolomitic limestones of the Yılanlı Formation. The purpose of the present s tudy was to describe the geological and mineralogical characteristics of K-bentonites exposed at the new localities, to present their chemical compositions in order to reveal the original geochemical affinities of their parental volcanic ash(es), to investigate their chemostratigraphic correlation based on immobile trace and *REE* compositions, with the previously discovered K-bentonite beds in the Bartın area, and, finally, to understand the tectonomagmatic setting of their source volcanoes.

LOCATION AND REGIONAL GEOLOGICAL SETTING OF THE STUDY AREA

The successions studied are included in the Zonguldak Terrane (ZT), one of main Palaeozoic tectonic units of Turkey (Fig. 1a,b). The regional geological setting and stratigraphy of the ZT have been described previously (Göncüoğlu *et al.*, 1997; Göncüoğlu & Kozlu, 2000; Yanev *et al.,* 2006). The basement rocks consist of Cadomian gneisses, gabbros, basalts, ultramafics and of pyroclastics, granites and felsic volcanic rocks. The basement rocks are overlain unconformably by Lower Ordovician units (Göncüoğlu *et al.* 2014), consisting of siltstones and mudstones (Bakacak Formation), and of conglomerates and sandstones (Kurtköy and Aydos formations) (Fig. 1c,d). The Upper Ordovician–Middle Silurian succession is represented by the Karadere, Ketencikdere and Fındıklı formations including graptolitic black and grey shales, with sandstones, siltstones (Schanski *et al.*, 2010) and limestone interlayers (Dean *et al.*, 1997) (Fig. 1d). The Fındıklı Formation is overlain unconformably by the Middle Devonian Bıçkı and Ferizli formations consisting of sandstones-mudstones and shales-siltstones, respectively. The Late Devonian–Early Carboniferous Yılanlı Formation, including shallow-marine dolomites and limestones, succeeds the Ferizli Formation (Aydın *et al.*, 1987; Derman 1997; Yalçın & Yılmaz, 2010; Bozkaya *et al.*, 2012). The Yılanlı Formation is ~800 m thick and consists of thick-bedded limestones, dolomitic limestones, and dolomites alternating with thin-bedded, black, calcareous shales. The transitional boundaries of the Yılanlı Formation with the Ferizli and Madendere formations were reported by Gedik *et al.* (2005). Based on fossil findings, Dil (1976) assigned a Middle Devonian–Early Carboniferous age for the Yılanlı Formation. The deposition of the Yılanlı Formation occurred mainly in an epeiric carbonate platform/shelf (Yalçın & Yılmaz, 2010). The Yılanlı Formation is overlain by a sequence, >500 m thick, of alternating limestones and shales (Fig. 1c, the Madendere and Karadon formations), followed by

https://doi.org/10.1180/claymin.2016.051.4.02 Published online by Cambridge University Press

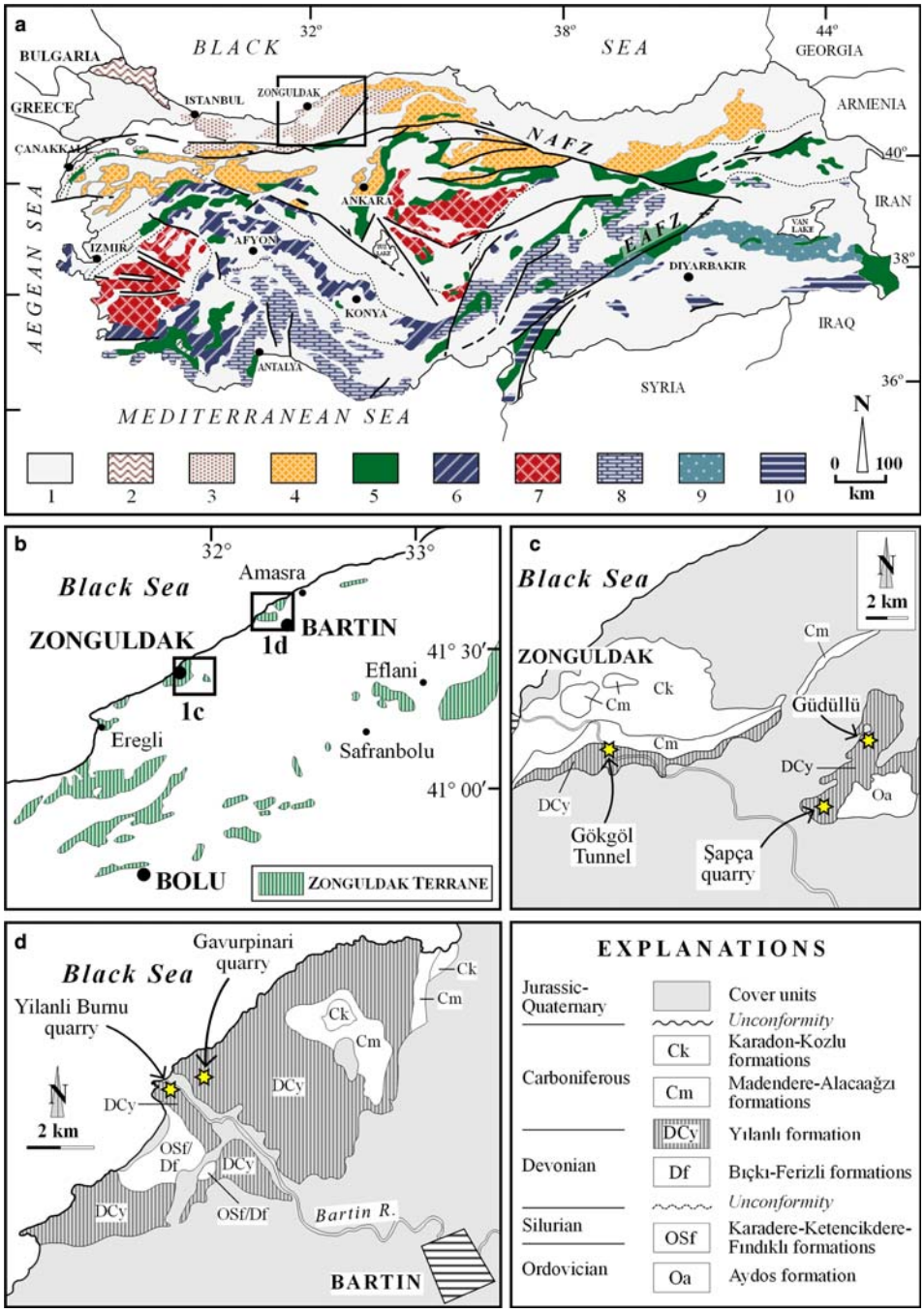

FIG. 1. (a) Alpine tectonic units of Turkey (Göncüoğlu *et al.*, 1997) and location of the İstanbul and Zonguldak terranes (NAFZ: North Anatolian Fault Zone, EAFZ: East Anatolian Fault Zone. Symbols: 1: Tertiary cover: 2: Istranca terrane, 3: İstanbul-Zonguldak terrane, 4: Sakarya composite terrane, 5: ophiolites and ophiolitic mélanges of Neotethyan suture belts, 6: Kütahya-Bolkardağ belt (Anatolides), 7: Menderes and Central Anatolian crystalline complexes (Anatolides), 8: Taurides, 9: Bitlis-Pötürge metamorphics (SE Anatolian autochthon), 10: SE Anatolian autochthon). (b) Distribution of Palaeozoic outcrops in the İstanbul and Zonguldak terranes (modified from Bozkaya *et al.*, 2012). (c–d) Geological maps of the study areas and geographical settings of sampling locations (modified from Akbaş *et al.*, 2002).

https://doi.org/10.1180/claymin.2016.051.4.02 Published online by Cambridge University Press

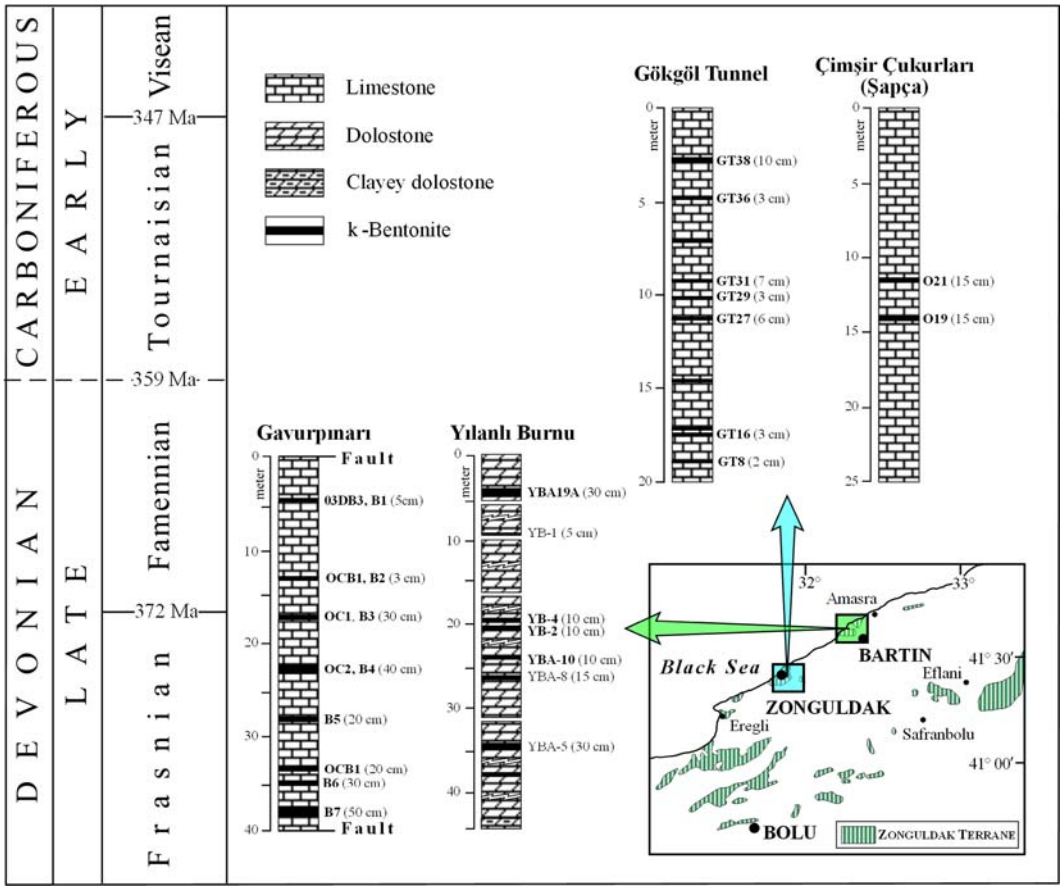

FIG. 2. Distribution of the Devonian–Carboniferous sequences of the Yılanlı Formation in NW Anatolia with the positions of the K-bentonite layers.

flood-plain deposits with numerous Westphalian-age coal-systems (Kerey, 1984).

The oldest cover of the Variscan units of the ZT are the Upper Permian (Tatarian) lagoonal sediments (Göncüoğlu *et al.,* 2011) to Upper Triassic continental red beds of the Çakraz Formation (Alişan & Derman, 1995). In addition, Cretaceous–Eocene formations are exposed in the study area.

DESCRIPTION OF THE K-BENTONITE BEDS EXPOSED IN THE STUDY AREA

The type locations of the new K-bentonite exposures within the upper levels of the Yılanlı Formation are at the limestone quarries near Güdüllü and Şapca villages and along the D750 highway at the southern entry of the Gökgöl tunnel road cuts between Zonguldak and Çaycuma cities (Fig. 1c). The geological details of the Bartın sections were given by Günal-Türkmenoğlu *et al.* (2012, 2015). In the present study only new fossil findings from this area are reported and the focus is mainly on the characteristics of the Şapca, Gökgöl Tunnel and Güdüllü outcrops. A composite log of the Yılanlı Formation is given in Fig. 2 for regional correlation.

Şapça area K-bentonite beds exposed in the Çimşir Çukurları limestone quarry

A number of limestone quarries exist within the outcrops of the Yılanlı Formation (DCy) between the Şapca and Güdüllü villages (Fig. 1c). Two K-bentonite beds exposed at Çimşir Çukurları east of Şapcı village,

https://doi.org/10.1180/claymin.2016.051.4.02 Published online by Cambridge University Press

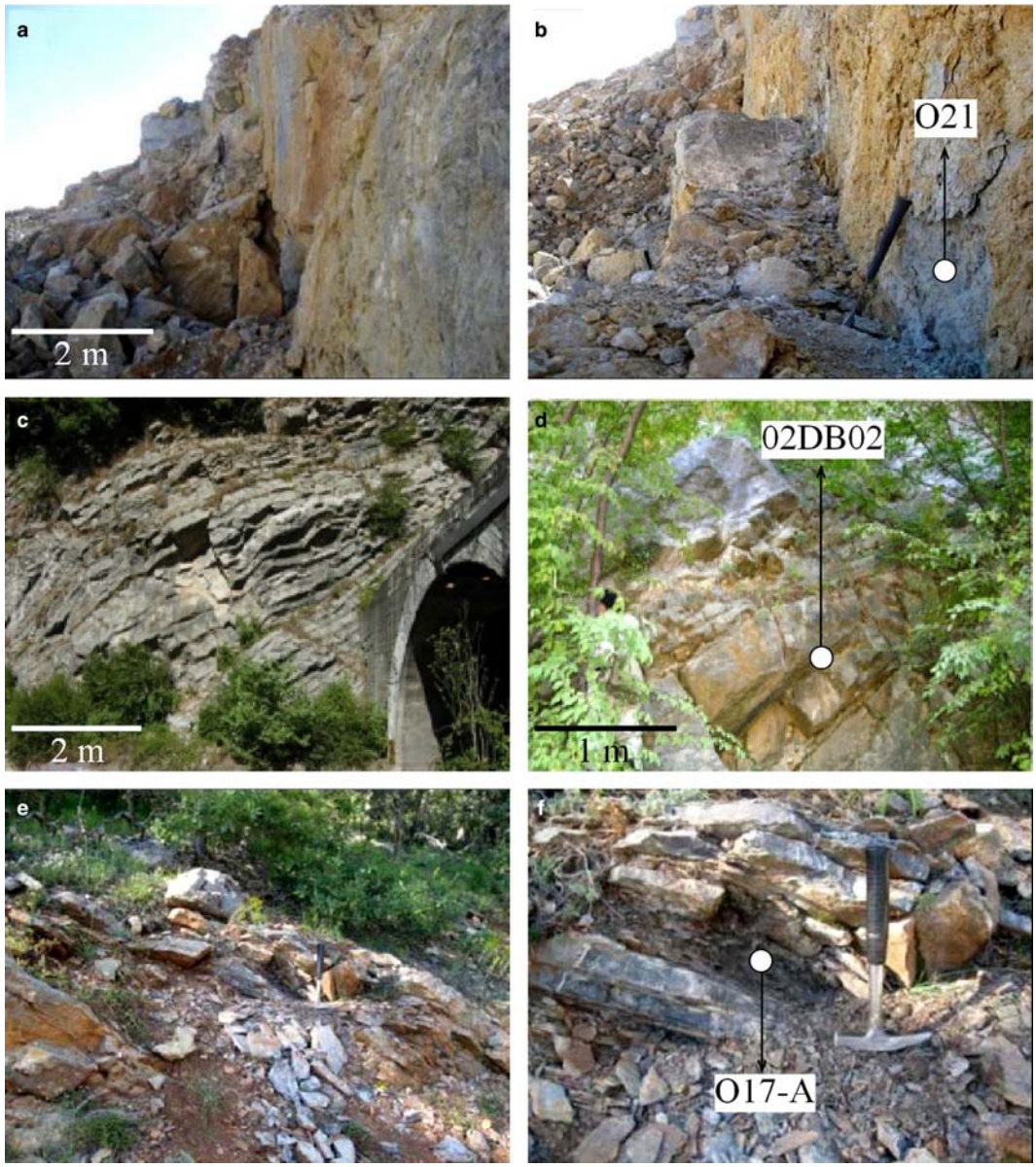

FIG. 3. (a) Vertical limestone beds interbedded with K-bentonite in Şapça Çimşir Çukurları quarry; (b) close-up view of the quarry face covered by a green to yellowish brown, fissile bentonite horizon lying parallel to the limestone bedding planes with a sharp contact; (c) Carboniferous limestone–clay interstratification at the Gökgöl highway tunnel entrance from Zonguldak; (d) close-up view of limestone lithologies interlayered with clay/bentonites; (e) field occurrence of limestone–clay/K-bentonite alternation in the Zonguldak-Güdüllü section; and (f) close-up view of K-bentonite in the Güdüllü section.

included in the 1:25,000 scale F27-b2 topographic map of Turkey, were studied. The limestone quarry has been excavated in three levels to a depth of >25 m from the topographic surface. The thick-bedded and grey Yılanlı Formation displays cracking and karstic dissolution voids. On the north side of the second

https://doi.org/10.1180/claymin.2016.051.4.02 Published online by Cambridge University Press

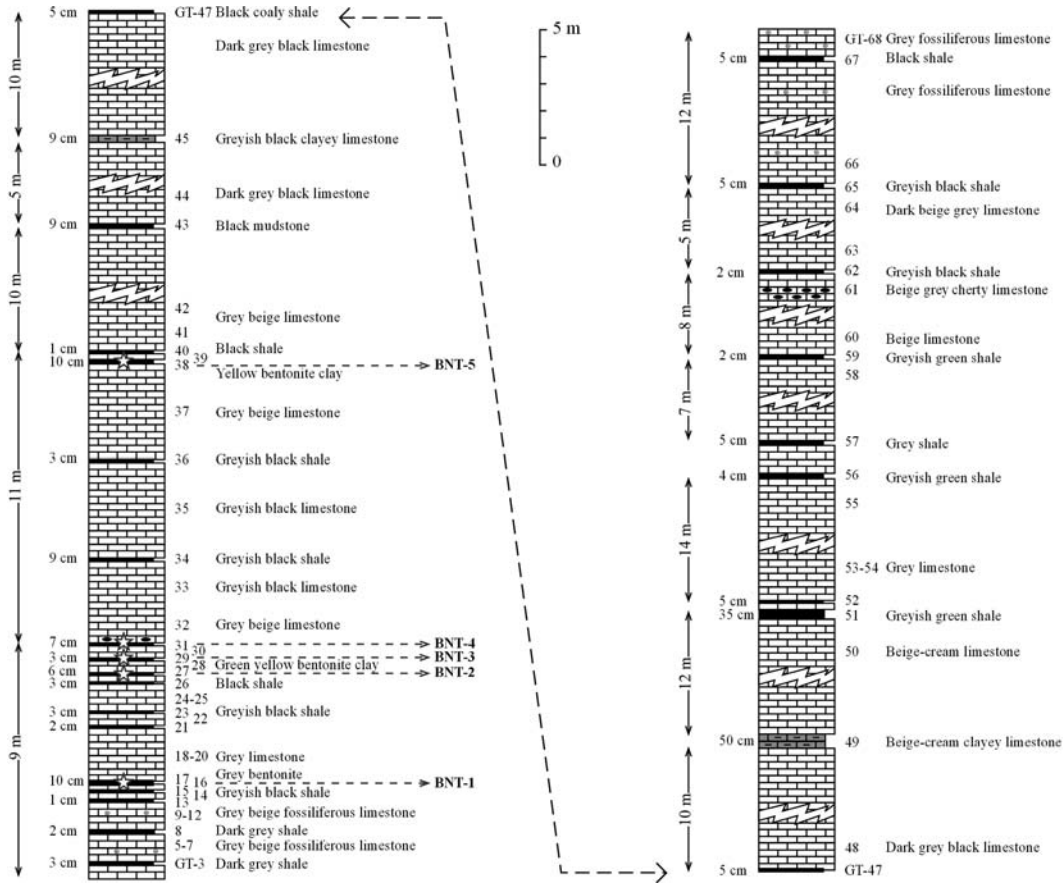

FIG. 4. Measured stratigraphic sections of limestone and clay/shale or bentonite layers along the Gökgöl tunnel section.

level of the quarry, at coordinates 31°56′53.19″ E/41° 25′13.26″N, limestone layers strike at N80°E with a dip of 70–80°N. At this section, ~50–60 cm of thick, grey limestone layers are interbedded with K-bentonite beds 10–15 cm thick (Figs 2, 3a,b). K-bentonites have characteristically light green colours when fresh but they become yellowish brown upon weathering. When wet they have a waxy, slippery and fissile texture. Because large amounts of block-size and smaller aggregate rock material was produced during mining activities, only two, mostly well exposed and prominent, bentonite beds were sampled and investigated (O19 and O21). These beds are found at both sides of a thick limestone bed which was also sampled in order to define their stratigraphic position within the Yılanlı Formation. The samples have abundant foraminiferal assemblages (mainly zonal taxa of quasiendothyrid and some specimens of endothyrid foraminifers) marking a relative age range at the Devonian–Carboniferous boundary, corresponding to Late Famennian–Early Tournaisian time.

K-bentonites from the Gökgöl highway tunnel section

Several cm-thick K-bentonite beds along the Gökgöl highway tunnel roadcut were discovered within the Middle Devonian–Lower Carbonifrous limestone-dolomitic limestone facies of the Yılanlı Formation. This location is included within the 1:25,000 scale F27-b1 topographic map of Turkey (Fig. 1c). The lower part of the Yılanlı Formation is faulted. Upwards, the Yılanlı Formation is overlain by the Namurian shale-mudstone-sandstone-coal sequences of the Alacaağzı formation. A 60 m-long section was measured in a NW to SE direction, starting from the south entrance of the highway tunnel, and clay and carbonate rock samples were collected (samples

https://doi.org/10.1180/claymin.2016.051.4.02 Published online by Cambridge University Press

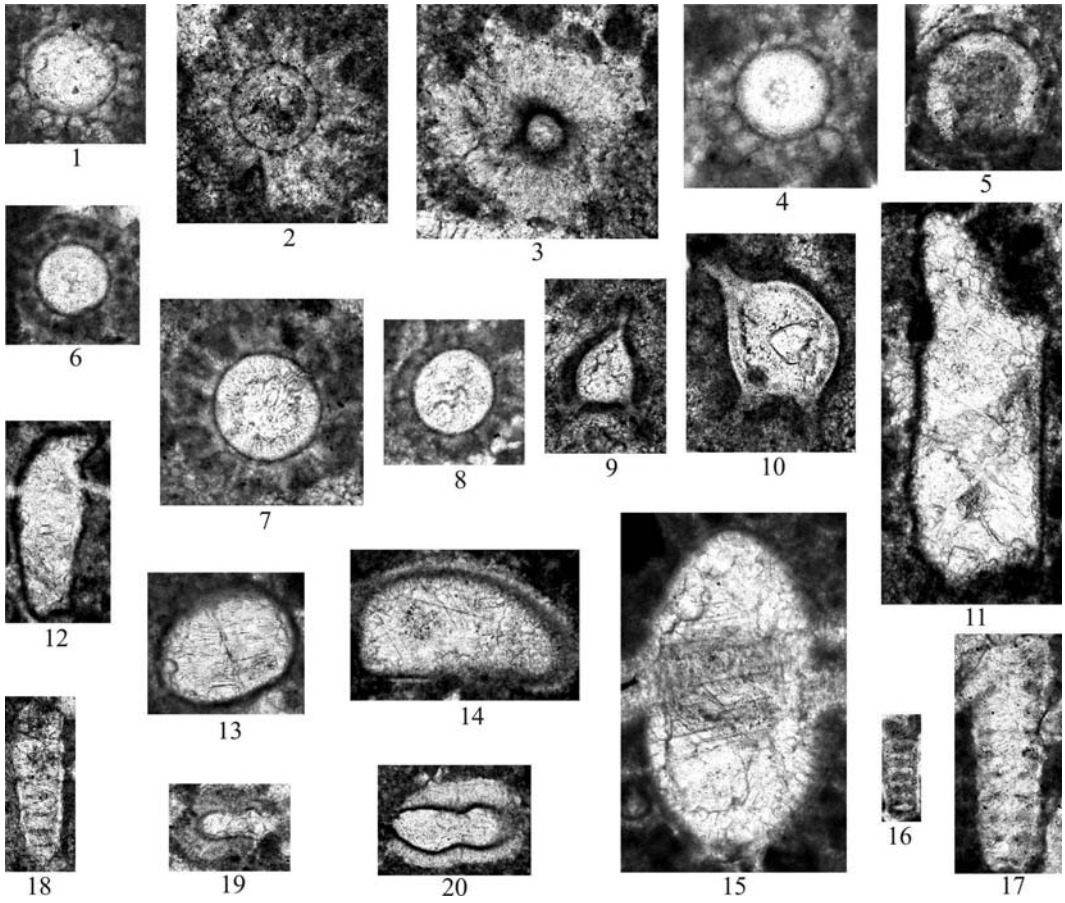

FIG. 5. Microfossils determined from the limestone-K-bentonite alternation in Yılanlı Formation at Gavurpınarı Quarry near Bartın: (1–4) *Radiosphaera* spp. ×105 [parts 1, 2, 03DLO03; Figs 3, 4, 04DLO03]; (5) *Tubeporina* sp., 03DLO03, ×105; (6–8) *Elenella* sp. ×105 [parts 6,7, 03DLO03, part 8, 04DLO03]; (9–10) *Parathurammina elegans* (Poyarkov, 1969), 03DLO03, ×105; (11–12) *Irregularina* spp., 04DLO03, ×60; (13–15) *Bisphaera elegans* (Vissarionova, 1950), ×60, [part 13, 03DLO03, parts 14–15, 04DLO03]; (16–18) *Eogeinitzina* (?) spp., axial sections, 03DLO03, ×60; (19–20) *Eogeinitzina* sp., transverse sections, ×60.

GT-1 to GT-68) (Figs 3c,d, 4). Similar facies are also exposed along the old service road to the west of the tunnel. The lower part of the measured section starts with cherty and fossiliferous micritic limestone layers, and continues upwards with an alternation of dark grey mudstone-greywacke lithologies including ostracod fossils with shale intercalations. During this investigation 2–20 cm thick, light grey to yellow K-bentonite beds were studied mainly for their geochemical characteristics. From bottom to top the bentonitic samples analysed included light brown-yellowish mudstone ~10 cm thick, at a height of 2.25 m (GT-16). This is overlain by thin organic shale which is covered by ~4 m of a fossiliferous, medium-bedded limestone sequence exhibiting alternating packstone-grainstone-wackestone facies. A second, light grey bentonitic bed with Fe-oxyhydroxides, with an average thickness of 6 cm was sampled (GT-27). The section continues upwards with grey-beige wackestone including abundant ostracod fossils. This layer is overlain by a black mudstone bed. The third bentonite horizon, 2 cm thick, was sampled ~7 m from the bottom of the measured section (GT-29). The fourth, yellow K-bentonite bed (GT-31) occurs at the 7.20 m level of the measured section and is separated from the previous one by mudstone-pelloidal pebblestone facies. The bed

https://doi.org/10.1180/claymin.2016.051.4.02 Published online by Cambridge University Press

includes chert fragments. The last yellowish brown bentonite bed (GT-38) along this measured section was sampled at 16 m from the bottom, and it appears after the accumulation of thick-bedded limestone layers alternating with thin shale-mudstone horizons. The measured section in the NW direction reaches the tunnel exit at a height of 60 m from the bottom (Figs 3c, d, 4). The upper part of the sequence is characterized by thick, fossil-rich limestone layers alternating with black-green clay-shale beds and represents a completely different facies from the K-bentonite-bearing succession that was studied. The finding of important fossils including foraminiferal taxa (*Quasiendothyra kobeitusana*, *Quasiendothyra communis*, *Quasiendothyra* ex gr. *konensis* and *Septatournayella* ex gr. *rauserae*) proves a Devonian–Carboniferous transitional age for the limestone layers adjacent to the K-bentonite beds under consideration.

K-bentonites from the Güdüllü area

This location is included within the 1:25,000 scale F27-b2 topographic map of Turkey at the SE of Güdüllü village and has the coordinates 32°00′27.56″ E/41°26′20.44″N (Fig. 1c). Two K-bentonite beds ~40 cm thick were observed within east-dipping, faulted and folded, dark-coloured limestone layers (Fig. 3e,f). A green clay bed, 30 cm thick, bounded by limestone layers, was sampled (O-17A) The limestone samples (O-18A and O-18B) yielded the same Late Devonian foraminiferal fossil assemblage as the K-bentonite-bearing succession in the upper part of the Yılanlı Formation cropping out at Gavurpınarı Quarry near Bartın, as studied previously (Günal-Türkmenoğlu *et al.*, 2015).

The age of the K-bentonite-bearing succession from the Gavurpınarı Quarry near Bartın is very definitive and rich collections of calcareous microfossils were recovered. The foraminiferal taxa are represented by *Parathurammina elegans* (Poyarkov, 1969), *Bisphaera elegans* (Vissarionova, 1950), *Radiosphaera* spp., *Tubeporina* sp., *Elenella* sp., *Irregularina* spp., *Eogeinitzina* sp. and *Eogeinitzina* (?) spp. (Günal-Türkmenoğlu *et al.*, 2015). Most are known widely, in many regions, and range stratigraphically from Devonian to Early Carboniferous (Dil, 1976; Vachard, 1991, 1994; Vachard *et al.*, 1994; Racki & Sobon-Podgorska, 1993; Kalvoda, 2001; Sabirov, 2004; Mamet & Preat, 2009; Özkan & Vachard, 2015) except for the age-diagnostic taxon, the multi-chambered foraminifer *Eogeinitzina* which is represented by only two transverse sections and three doubtful specimens (Fig. 5). *Eogeinitzina* is one of the important index Frasnian genera of the multilocular foraminifera (nodosariids) and allows a worldwide correlation of the Frasnian, especially late-Frasnian carbonate sequences (Dil, 1976; Vachard, 1991, 1994; Vachard *et al.*, 1994; Racki & Sobon-Podgorska, 1993; Kalvoda, 2001; Sabirov, 2004).

ANALYTICAL METHODS

The K-bentonite samples and associated carbonate rocks were investigated by optical microscopy and X-ray diffraction (XRD) to identify textural properties, non-clay and clay mineral components in the Optical-, Clay-Mineralogy and XRD Laboratories at the Geological Engineering Department of Middle East Technical University. The samples were X-rayed using a Rigaku Miniflex II diffractometer with Ni-filtered Cu$K\alpha$ radiation and a graphite monochromator at 35 kV and 15 mA with a scanning speed of 2°/min and 1°/min for mineral identification and for determination of the Kübler Index of illite (Kisch, 1991). Non-clay minerals were identified from randomly oriented powders obtained by agate mortar, and sieved below 90 μm (170 mesh) without any chemical treatment. Clay fractions (grain size of <2 μm) were separated by dispersing the bulk sample in distilled water after treatment with NaOAc buffer for dissolution of carbonates, followed by sedimentation and centrifugation (Jackson, 1969). Oriented mounts were obtained by thinly smeared clay pastes on glass slides. The XRD patterns were obtained after air-drying, ethylene-glycol (EG) solvation and heating at 550°C. Determination of clay minerals from XRD patterns followed Brown & Brindley (1980), Hoffman & Hower (1979) and Moore & Reynolds (1997).

The Kübler Index (KI, Kübler, 1968; Guggenheim *et al.*, 2002) was determined by measuring the full width at half maximum (FWHM) at the first basal illite reflection near 10 Å in air-dried samples. Crystallinity Index Standards (CIS, Warr & Rice, 1994) were used to calibrate the FWHM values. The CIS values were re-calibrated with the equation of Warr & Ferreiro Mahlmann (2015) to convert the original upper and lower boundary limits of anchizone, 0.25°2θ and 0.42°2θ (Kübler, 1967). The d_{060} values of illite were identified in the range 59–63°2θ using quartz as an internal standard. The octahedral Fe+Mg contents (atoms per formula unit, a.p.f.u.) of illite were estimated from the equation of Guidotti *et al.* (1992). Illite polytypes were identified at characteristic peaks (16–36°2θ) from random preparations (Bailey, 1988),

https://doi.org/10.1180/claymin.2016.051.4.02 Published online by Cambridge University Press

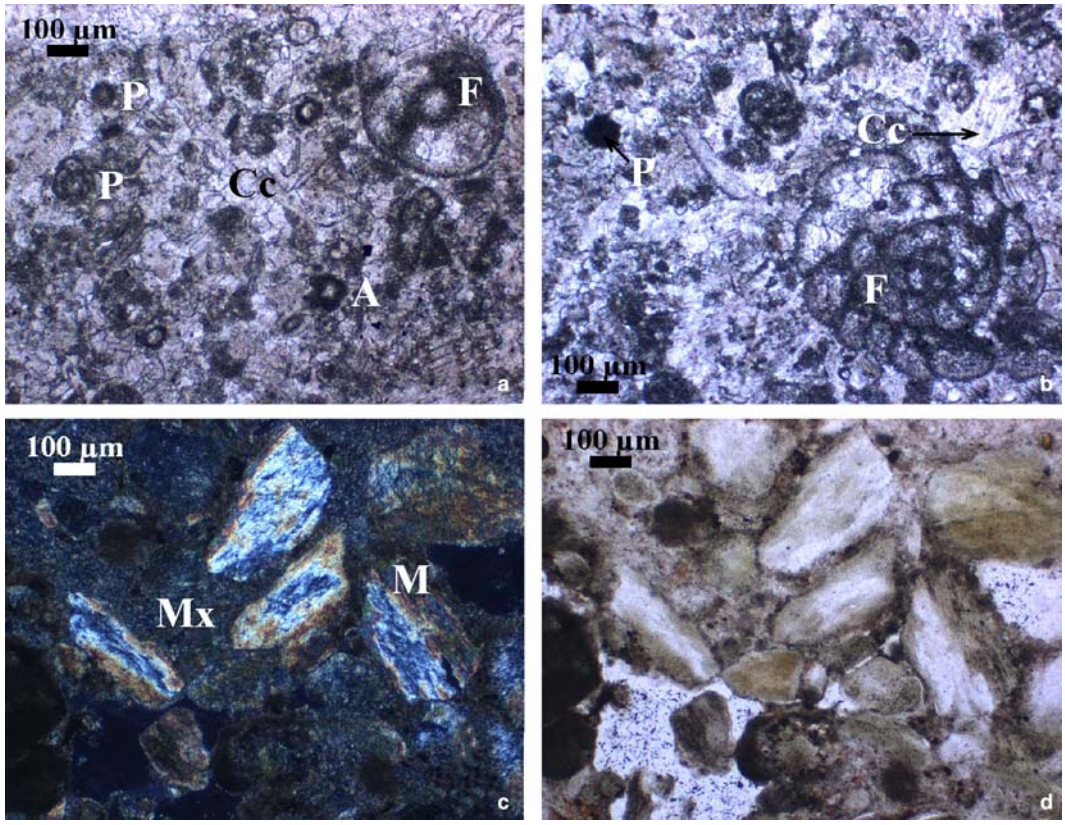

FIG. 6. Photomicrographs of the limestone facies from Çimşir Çukurları quarry in the Şapça area: (a–b) Grainstone facies with benthic foraminifera (mainly quasiendothyrid) (plain polarized light, ppl); (c–d) K-bentonite sample with highly altered mineral (feldspar) crystals in a calcareous-clayey matrix (part c – crossed nicols – cn, part d – ppl) (F: Foraminifera, P: Pellet, Cc: Calcite cement, A: Algae, M: Mineral, Mx: Matrix).

using the A(2.80)/A(2.58) and A(3.07)/A(2.58) peak area ratios (Grathoff & Moore, 1996).

The chemical compositions of the bulk K-bentonite samples (major, trace and rare earth elements) were determined by inductively coupled plasma-mass spectrometry (ICP-MS) in ACME Analytical Laboratories Ltd. (Vancouver, Canada).

RESULTS AND DISCUSSION

Depositional environment of K-bentonites

The carbonate rocks of the Yılanlı Formation in contact with K-bentonite beds at the Şapca area consist of benthic foraminifera-bearing pelloidal grainstone facies and contain small amounts of algal components (Fig. 6a,b). The presence of abundant foraminifera and pellets indicates a tidal depositional environment. The K-bentonite bed (Sample No. O19), which is interlayered with this carbonate facies, has abundant mineral crystals embedded in a clayey matrix (Fig. 6c,d). The mineral fragments consist mainly of highly altered feldspar grains.

The Yılanlı Formation in the Güdüllü area shows a wide variation of carbonate facies along the sequence (Fig. 7). Mudstone-packstone-wackestone facies alternations are abundant at the bottom. The intercalation of packstone-wackestone facies includes bioclastic and intraclastic content with brachiopods, ostracods and corals. The presence of dolostone facies indicates changes in the depositional environment and the effects of diagenesis. At the top of the sequence, boundstone-wackestone carbonate facies include benthic foraminifers and brachiopods, and laminations, in addition to bird's eye textures. Mudstone intercalations are common. These facies changes

https://doi.org/10.1180/claymin.2016.051.4.02 Published online by Cambridge University Press

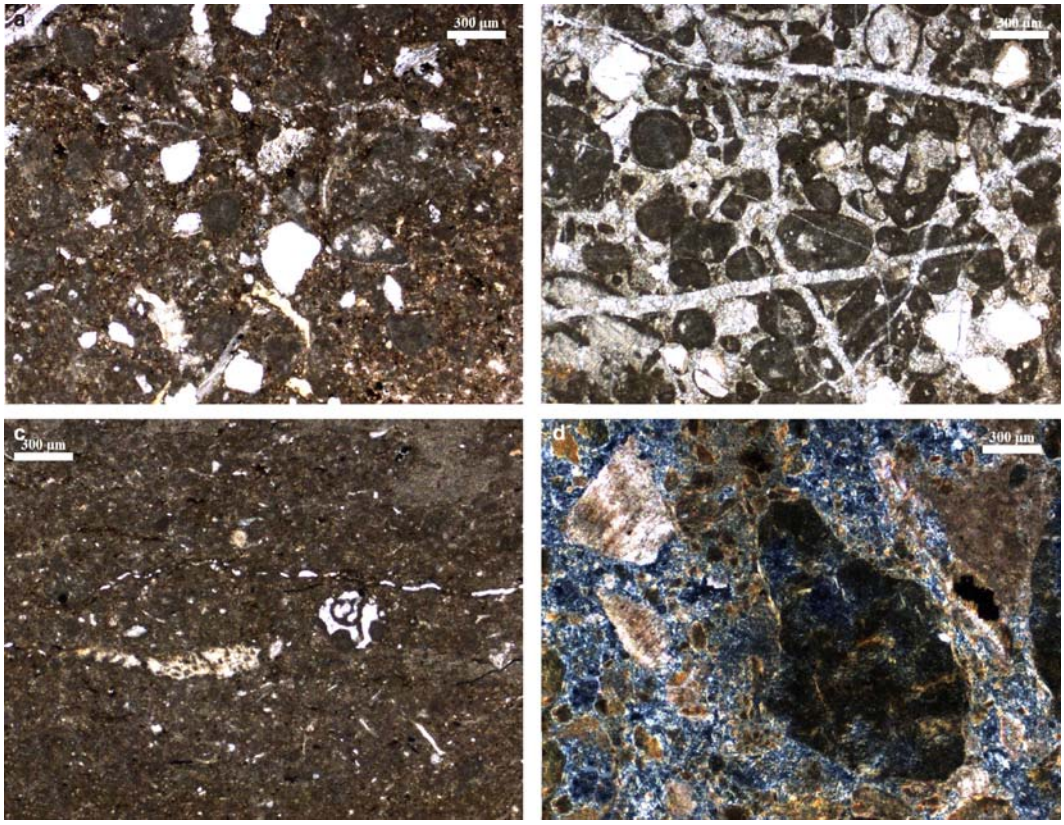

FIG. 7. Photomicrographs of limestone facies from the Güdüllü area: (a) wackestone facies with quartz, ostracods and siliceous grains (ppl); (b) grainstone facies with ooids and intraclasts (ppl); (c) boundstone-wackestone facies including lamination, bird's eye texture, foraminifera and brachiopoda (ppl); and (d) mudstone facies including highly altered K-bentonite sample with highly argillized grains (cn).

reflect frequently changing environmental conditions and shallowing upwards.

An ostracod- and bivalve-rich facies in depositional contact with the overlying K-bentonite layers was observed during field studies. The carbonate facies overlying the K-bentonites directly are fossil-free, however, and may belong to a different facies-type of pelloidal packstone. The first organic remains were observed at ~10 cm above the top of the K-bentonite layer. Hence, it is assumed that the tephra deposition on the sea bottom may have affected the living conditions of marine organisms causing a local mass extinction for a short period.

Mineralogical characterization of K-bentonites

The major non-clay minerals in the K-bentonite samples are quartz, calcite and dolomite (Fig. 8). Minor minerals are plagioclase, anatase, pyrite, gypsum, goethite and alunite. Fine zircon crystals were only observed during optical investigations. The clay content of the samples varies between 70 and 94%. In the clay fractions, illite is the major clay mineral in the Gavurpınarı and Yılanlı Burnu quarry samples, and the dominant mineral in the Güdüllü samples (*e.g.* 90% illite and 10% mixed-layer illite-smectite in sample O-17A). In contrast, the clay fractions of the samples from Şapca-Çimşir Çukurları and Gökgöl tunnel sections contain 98–100% R1- and R3-type (Moore & Reynolds, 1997) mixed-layer illite-smectite (I-S) and up to 2% kaolinite (Fig. 8). The mineralogical data suggest that the illite-rich Gavurpınarı, Yılanlı Burnu and Güdüllü samples were affected by higher-degree diagenetic conditions compared to the I-S rich samples from the Şapca and Gökgöl tunnel locations (Table 2, Fig. 9). The d_{060}

https://doi.org/10.1180/claymin.2016.051.4.02 Published online by Cambridge University Press

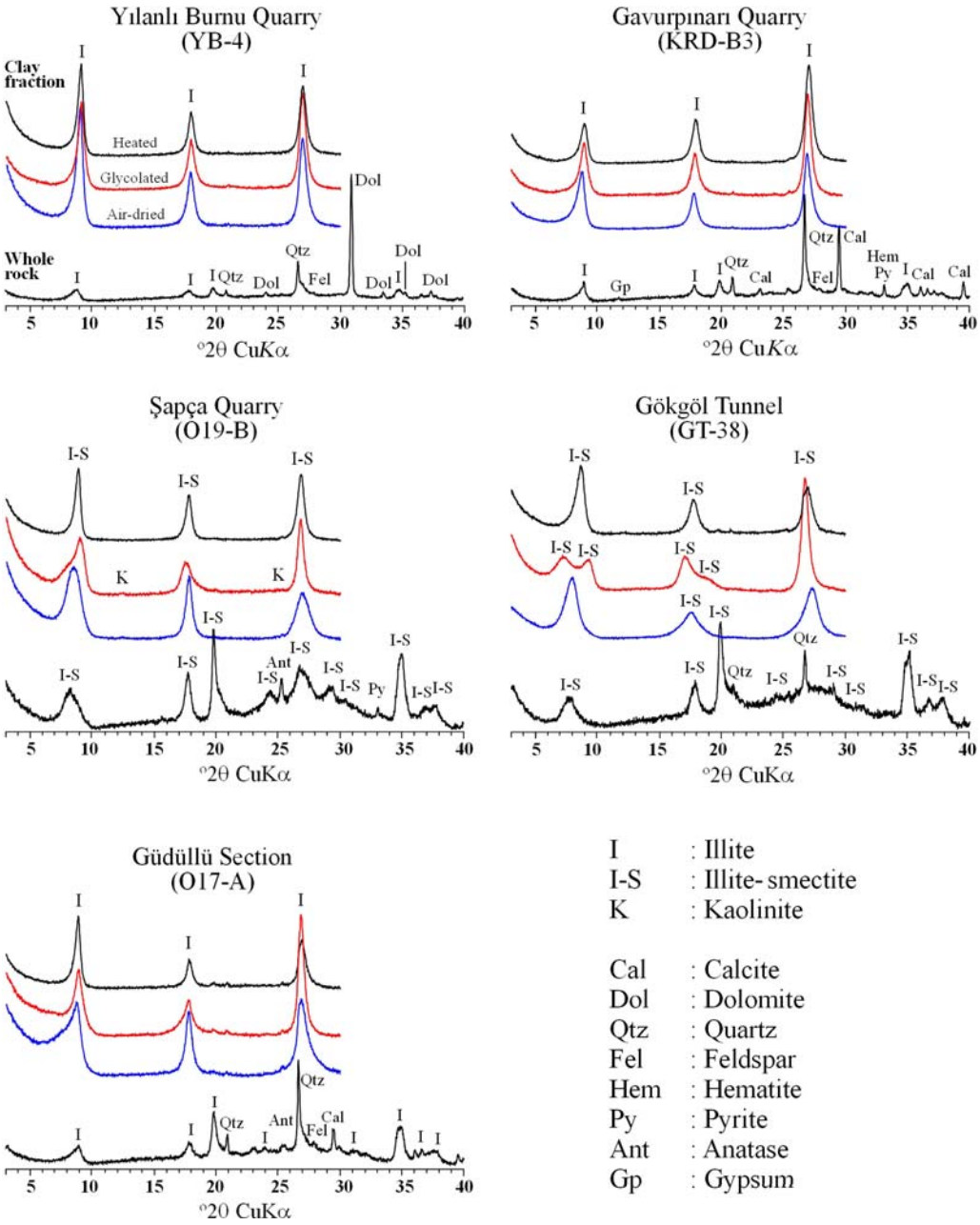

FIG. 8. XRD patterns of bulk and clay fractions of the representative K-bentonite samples from different areas.

values of illites of the Yılanlı Burnu and Gavurpınarı quarries indicate compositions between ideal muscovite and phengite (octahedral Mg+Fe = 0.08–0.61 a.p.f.u), whereas those of I-S of Çimşir Çukurları quarry and Gökgöl Tunnel have muscovitic composition (octahedral Mg+Fe < 0.06 a.p.f.u). Higher d_{060} values for the Yılanlı Burnu quarry were observed in bentonites associated with dolomitic rocks. Illite polytypes are represented by $2M_1 + 1M_d$, whereas R3 and R1 I-S exhibit $1M_d$ polytypes only (Fig. 9).

https://doi.org/10.1180/claymin.2016.051.4.02 Published online by Cambridge University Press

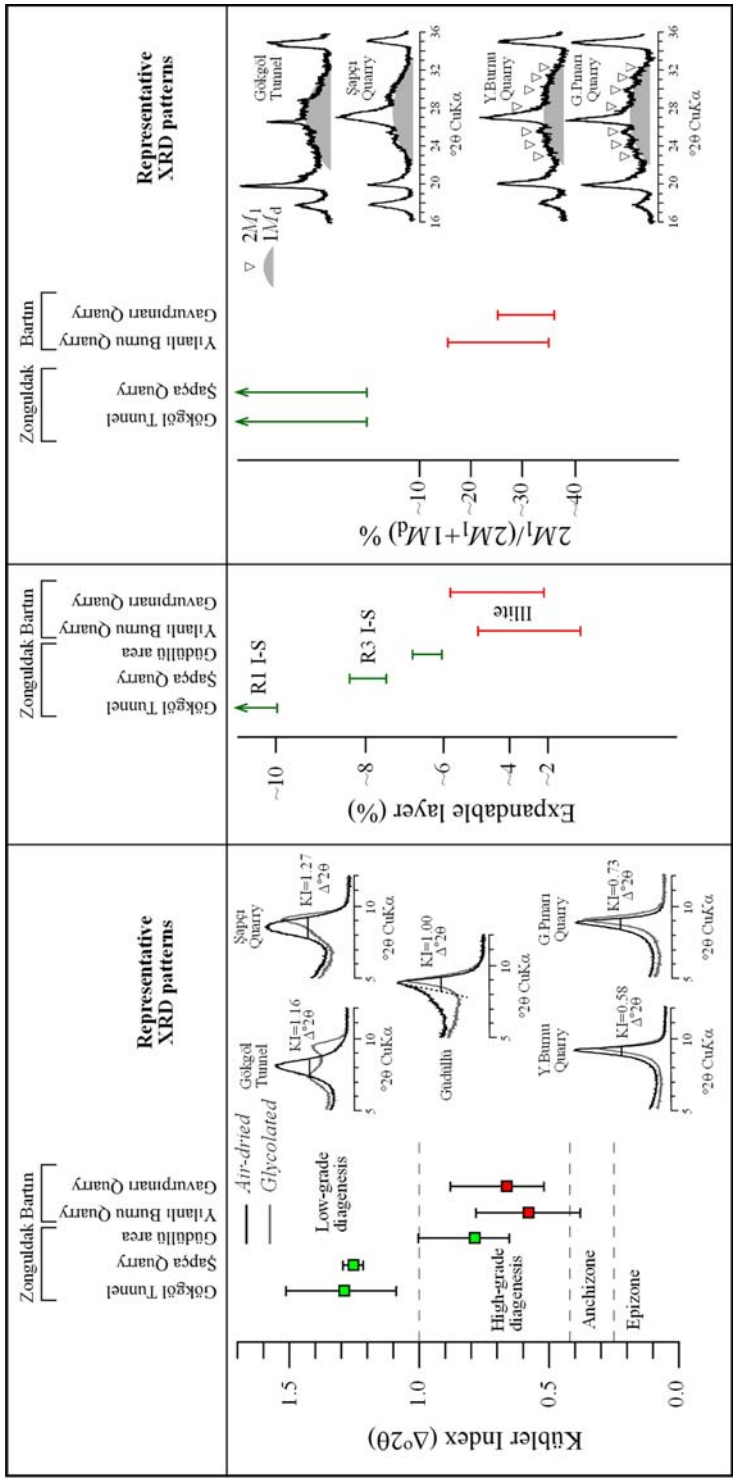

FIG. 9. Main mineralogical characteristics of illites and I-S in K-bentonite samples from different areas.

https://doi.org/10.1180/claymin.2016.051.4.02 Published online by Cambridge University Press

Illitization is affected by several factors including the increase in temperature during progressive burial, the geotectonic regime, the period of heating, the rock composition, K^+ availibility and fluid circulation (Frey, 1987; Merriman & Peacor, 1999; Árkai *et al.*, 2002; Dellisanti *et al.*, 2008). Alternatively, Merriman & Frey (1999) indicated that accretionary burial of young strata beneath older strata produces characteristic patterns of metamorphic grade increasing into sequentially younger rocks. According to Christidis *et al.* (1995) the Lower Pleistocene bentonite deposits of eastern Milos, Greece which formed by the submarine alteration of volcanoclastic rocks, erupted from different centres. During the alteration by sea water of parental rocks to smectite-rich bentonites, leaching and removal of major elements such as Na, K and Ca took place. The source of Fe and Mg was the parent rock and uptake from sea water should be limited. The study by Christidis *et al.* (1995) showed the role of different parent-rock compositions in the origin of smectite by the process of alteration of volcanic glass.

The present study showed the existence of two different degrees of illitization corresponding to the K-bentonites from the Güdüllü and Şapca-Gökgöl tunnel locations. The inherited geochemical features of these bentonites as discussed in the paragraphs below also relate these two mineralogical assemblages to different parent-rock compositions. These data may imply that the illitization processes during the evolution of K-bentonites was also affected by parent-rock compositions.

Geochemical fingerprinting of the K-bentonites

K-bentonite layers are extremely important stratigraphic marker beds. The elemental geochemical compositions not only make possible the regional correlation of marker beds over wide areas, but they also provide information about the chemical characteristics of the parent magma and the tectonomagmatic setting of the source volcanoes (Ver Straeten, 2004). Because K-bentonites evolve mainly by the alteration of original tephra deposits, TiO_2, and high field strength (HFS) elements (Zr, Nb, Hf, Ta and *REE*) tend to be immobile and remain uneffected by diagenesis and low-grade metamorphism, and thus are used primarily for extracting information about their original magma chemistry (Huff & Türkmenoğlu, 1981; Teale & Spears, 1986; Merriman & Roberts, 1990; Huff *et al.*, 1997; Histon *et al.,* 2007). A discrimination plot of Zr/TiO_2 *vs*. Nb/Y (Winchester & Floyd, 1977) may give information on the original composition of the parent magma of the volcanism producing the tephra studied. In addition, explosively erupted volcanic ashes have silicic compositions and are rich in volatiles (H_2O), as also reflected by moderate to high Nb and Zr contents (Izett, 1981). N-MORB-normalized trace-element data and chondrite-normalized *REE* data plots have been used to understand the compositions of source magmas and their volcanic environmental settings (Taylor & McLennan, 1988).

Geochemical data from the present study, on a total of 22 field samples (Table 3), were evaluated and compared with the whole-rock major, trace and rare earth element compositions. Eight are from the Şapca, Güdüllü and Gökgöl tunnel areas. Nine samples were taken recently from the previously investigated Gavurpınarı and Yılanlı Burnu quarries in the Bartın area for geochemical correlation. In addition, previous geochemical data (Günal-Türkmenoğlu *et al.*, 2015) from five Devonian K-bentonites from the latter quarries are also included for correlation. In this way,

Table 1. Locations of the K-bentonite samples.

Sample No	Location	Reference
OC1*, OCB1*, 03DB03, B1, B2, B3, B4, B5, B6, B7	Gavurpınarı quarry, Bartın	*Günal-Türkmenoğlu *et al.* (2015)
YBA19A*, YB4*, YB2*, YBA10	Yılanlı Burnu quarry, Bartın	*Günal-Türkmenoğlu *et al.* (2015)
O19, O21	Çimşir Çukurları quarry, Şapca	Present study
O17A	Güdüllü (Çukurören village)	Present study
GT16, GT27, GT29, GT31, GT38	Gökgöl highway tunnel roadcut	Present study

https://doi.org/10.1180/claymin.2016.051.4.02 Published online by Cambridge University Press

TABLE 2. Crystal-chemical characteristics of illite and I-S in K-bentonites.

	Mineral composition		Crystal-chemical data			
	Bulk	Clay	KI (Δ°2θ)*	d_{060} (Å)	$2M_1$	$1M_d$
Yılanli Burnu quarry	Dol±Qz±Fsp+Clay	Ilt±Kln	0.38–0.78 (0.58)	1.4992–1.5039 (1.5012)	15–35 (25)	60–80 (75)
Gavurpinari quarry	Cal+Qz±Dol+Clay	Ilt±Kln	0.52–0.88 (0.66)	1.4991–1.5015 (1.5000)	25–35 (32)	65–75 (68)
Çukurören village	Cal+Qz+Clay	Ilt±I-S	0.65–0.92 (0.78)	1.5000	40	60
Şapçı quarry	Clay±Cal	I-S (R3)	1.24–1.27 (1.26)	1.4967–1.4972 (1.4970)	–	100
Gökgöl tunnel	Clay±Cal	I-S (R1)	1.09–1.52 (1.33)	1.4987–1.4989 (1.4988)	–	100

Cal, Calcite; Dol, Dolomite; Qz, Quartz; Fsp, Feldspar; Ilt, Illite; Kln, Kaolinite; I-S, mixed-layer illite-smectite.

TABLE 3. Major, trace and rare earth element analysis of K-bentonite samples.

Sample	OC1	OCB1	03DB03	B1	B2	B3	B4	B5	B6	B7	YBA19A
Wt.%											
SiO_2	58.64	52.85	54.98	16.13	35.06	36.02	54.20	47.91	47.75	35.91	38.74
Al_2O_3	21.50	18.53	20.95	5.73	10.69	12.88	21.23	17.19	17.99	15.26	14.35
Fe_2O_3	2.45	8.76	2.33	1.71	4.53	2.69	2.97	8.49	3.73	4.69	4.79
MgO	0.90	2.65	1.14	1.12	1.50	1.87	2.87	2.42	5.06	2.18	8.53
CaO	0.83	1.28	4.78	39.33	22.10	20.76	1.32	5.76	5.27	16.83	8.62
Na_2O	0.11	0.10	0.10	0.02	0.05	0.08	0.11	0.09	0.10	0.08	0.08
K_2O	2.66	6.01	2.88	1.77	3.34	4.15	6.80	5.49	5.74	4.88	5.91
TiO_2	1.20	0.94	1.22	0.21	0.50	0.59	1.08	0.87	0.88	0.78	0.42
P_2O_5	0.05	0.28	0.18	0.04	0.13	0.18	0.27	0.23	0.23	0.20	0.10
MnO	<0.01	<0.01	<0.01	<0.01	<0.01	<0.01	<0.01	<0.01	<0.01	<0.01	0.02
Cr_2O_3	0.021	0.016	0.022	0.05	0.010	0.011	0.018	0.015	0.016	0.014	0.011
LOI	11.5	8.4	11.3	33.8	21.9	20.6	8.9	11.3	13.0	19.0	18.2
Sum	99.86	99.82	99.84	99.92	99.82	99.83	99.74	99.75	99.76	99.81	99.77

(continued)

TABLE 3. (*contd.*)

Sample	OC1	OCB1	03DB03	B1	B2	B3	B4	B5	B6	B7	YBA19A
ppm											
Ni	26	50	71	<20	<20	33	51	60	30	45	41
Sc	20	16	20	4	8	11	19	15	15	14	13
Ba	385	258	334	49	136	190	312	244	265	210	159
Be	5	4	1	1	2	3	5	4	3	3	<1
Co	2.7	10.8	10.4	3.3	6.3	14.7	17.2	14.1	8.2	8.2	10.09
Cs	23.1	13	20.10	3.9	6.8	8.4	15.0	14.1	12.1	17.6.	0.8
Ga	24.9	23.4	24.2	6.0	13.5	15.4	25.8	20.3	22.5	17.3	17.9
Hf	6.2	6.4	6.5	0.9	2.5	2.9	6.1	4.8	4.7	4.1	1.1
Nb	21.8	20.6	20.5	5.1	11.0	14.7	24.9	20.4	23.8	17.5	7.3
Rb	120.2	210.1	119.7	55.9	115.5	149.5	247.6	193.0	193.5	173.2	163.8
Sn	4	3	3	3	3	4	4	6	3	5	2
Sr	75.4	171.5	249.5	172.2	653.1	389.9	468.2	443.2	268.8	502.1	241.6
Ta	1.4	1.3	1.5	0.3	0.7	0.8	1.6	1.3	1.3	1.2	0.5
Th	12.2	14.2	17.0	3.7	8.6	10.5	19.5	15.6	17.0	14.3	6.5
U	4.2	8.8	5.0	2.2	4.9	6.4	9.6	8.5	9.6	6.1	10.3
V	198	148	203	45	94	147	139	181	152	173	97
W	3.2	3.2	3.6	1.0	4.9	2.5	4.2	3.9	5.4	5.0	1.0
Zr	216.5	172.8	227.9	38.9	80.8	102.3	208.5	177.1	177.1	148.1	38.8
Y	18.7	21.6	25.4	3.9	5.0	9.6	19.7	15.5	13.3	14.0	9.7
La	32.3	35.6	35.2	8.1	17.0	20.0	39.6	33.6	30.3	26.8	20.2
Ce	55.2	76.1	73.0	16.0	32.0	41.0	89.1	75.7	66.5	60.4	35.0
Pr	6.03	9.10	8.19	1.69	3.36	4.54	9.94	8.15	6.85	6.45	3.94
Nd	21.8	33.3	29.3	6.1	10.6	16.0	35.9	30.6	24.1	22.7	12.9
Sm	3.43	6.34	5.37	1.01	1.62	2.99	6.53	5.37	4.15	4.13	2.64
Eu	0.67	1.19	1.14	0.22	0.28	0.55	1.25	0.97	0.75	0.76	0.53
Gd	2.61	5.01	4.23	0.79	0.89	2.16	4.92	3.85	3.03	3.03	2.25
Tb	0.45	0.75	0.72	0.14	0.40	0.34	0.76	0.58	0.50	0.53	0.34
Dy	3.01	4.42	4.48	0.64	0.87	1.74	3.86	3.27	2.79	2.79	2.04
Ho	0.66	0.79	0.89	0.14	0.20	0.37	0.78	0.63	0.58	0.57	0.38
Er	2.32	2.24	2.75	0.38	0.60	1.15	2.42	1.89	1.68	1.71	0.99
Tm	0.37	0.35	0.44	0.08	0.11	0.18	0.37	0.31	0.28	0.28	0.16
Yb	2.66	2.39	3.09	0.47	0.84	1.15	2.50	2.01	1.69	1.80	1.11
Lu	0.40	0.34	0.43	0.06	0.12	0.18	0.39	0.31	0.29	0.25	0.16

TABLE 3. (*contd.*)

Sample	YB4	YB2	YBA10	O19	O21	O17A	GT16	GT27	GT29	GT31	GT38
SiO_2	42.40	44.26	40.22	44.18	38.38	52.99	47.43	42.25	48.99	51.34	52.27
Al_2O_3	14.32	15.00	13.39	26.15	20.55	20.33	20.17	16.68	17.57	21.08	21.28
Fe_2O_3	3.60	3.95	3.64	3.36	2.89	3.66	3.60	3.71	7.22	2.03	1.91
MgO	9.16	8.12	9.53	2.02	2.21	4.46	3.57	3.40	3.67	4.34	4.30
CaO	6.93	6.05	8.42	4.32	12.46	1.59	4.67	11.11	3.85	2.61	0.90
Na_2O	0.05	0.06	0.06	0.12	0.04	0.11	0.03	0.04	0.04	0.02	0.02
K_2O	5.80	5.81	5.46	6.59	5.63	6.88	5.66	5.24	5.39	5.65	5.60
TiO_2	0.44	0.62	0.55	1.41	0.98	0.47	1.07	0.95	0.90	0.44	0.43
P_2O_5	0.04	0.06	0.05	0.10	0.13	0.07	0.06	0.02	0.04	0.01	<0.01
MnO	0.02	0.01	0.01	<0.01	<0.01	0.01	0.02	0.02	0.02	<0.01	<0.01
Cr_2O_3	0.010	0.012	0.011	0.006	0.005	0.014	0.002	<0.002	0.007	<0.002	<0.002
LOI	17.0	15.8	18.5	11.1	16.5	9.3	13.4	16.3	11.9	12.2	12.14
Sum	99.80	99.79	99.79	99.35	99.73	99.87	99.96	99.71	99.60	99.75	99.74
ppm	28	29	42	79	56	23	<0.20	<0.20	<0.20	<0.20	<0.20
Ni	10	10	10	13	3	18	5	6	11	5	6
Sc	81	93	81	33	27	261	33	37	98	20	19
Ba	3	2	2	5	3	4	3	7	4	31	3
Be	8.9	6.0	4.9	2.4	2.1	6.3	0.3	2.5	4.46	0.3	<0.2
Co	11.5	12.6	12.1	11.5	15.2	17.3	20.6	13.5	20.4	21.0	31.3
Cs	18.0	21.9	17.9	25.1	21.6	24.6	27.7	32.3	36.6	41.7	47.2
Ga	2.5	3.2	2.9	59.5	19.7	1.2	27.8	22.7	37.0	30.0	33.0
Hf	9.4	12.0	10.6	408.9	184.7	9.0	209.6	198.8	262.9	155.0	163.7
Nb	197.2	198.7	182.6	130.9	135.3	268.8	147.6	148.4	207.9	151.8	159.3
Rb	2	3	1	7	2	3	5	4	8	5	4
Sn	68.1	162.6	122.0	274.6	84.1	37.5	189.6	172.7	57.0	30.9	19.6
Sr	0.6	0.9	0.8	24.1	5.3	0.7	15.7	12.5	17.0	9.9	10.7
Ta	9.3	12.3	10.5	70.5	33.8	8.2	25.3	18.3	30.3	38.2	45.6
Th	3.6	6.6	5.1	38.3	24.8	1.8	16.4	5.6	4.5	1.2	1.7
U	90	98	81	3i2	195	126	27	27	82	13	<8
V	1.2	1.6	1.4	3.5	2.6	1.6	5.4	2.4	2.7	1.7	1.0
W	79.5	112.5	99.9	2282.1	939.7	39.0	1085.0	927.4	1530.4	917.1	968.4
Zr	5.4	6.1	6.3	154.3	40.3	7.1	27.5	32.9	20.8	14.9	15.5

(continued)

TABLE 3. (*contd.*)

Sample	YB4	YB2	YBA10	O19	O21	O17A	GT16	GT27	GT29	GT31	GT38
Y	14.9	20.4	17.7	208.0	36.5	16.9	94.6	48.3	15.5	5.1	8.0
La	23.1	31.8	29.6	417.4	53.0	32.1	205.7	108.6	39.9	15.6	23.2
Ce	2.46	3.24	3.13	46.37	6.67	3.83	22.75	13.07	6.78	2.86	4.04
Pr	8.4	9.7	11.1	142.3	25.0	13.9	74.8	48.9	31.3	12.8	18.6
Nd	1.28	1.52	1.67	29.69	5.52	2.7	14.22	9.92	7.28	3.22	4.04
Sm	0.2	0.24	0.26	5.07	1.44	0.45	2.77	1.91	1.29	0.38	0.42
Eu	0.87	0.95	1.24	27.91	5.73	2.01	10.08	7.55	5.67	2.61	3.11
Gd	0.14	0.17	0.19	4.90	0.90	0.31	1.40	1.23	0.84	0.49	0.53
Tb	0.82	1.27	1.05	28.18	5.10	1.65	7.01	7.11	4.32	2.98	2.72
Dy	0.2	0.22	0.24	5.39	1.03	0.28	1.09	1.25	0.76	0.60	0.48
Ho	0.61	0.78	0.72	14.54	2.70	0.85	2.74	3.31	2.09	1.76	1.36
Er	0.10	0.13	0.13	2.00	0.35	0.15	0.38	0.50	0.33	0.26	0.21
Tm	0.69	1.08	0.97	11.97	2.11	1.02	2.35	3.14	2.34	1.83	1.43
Yb	0.11	0.14	0.15	1.67	0.30	0.15	0.30	0.45	0.38	0.27	0.21

the comparison of the magma chemistry, tectonic setting and stratigraphic range of K-bentonites from these two different areas, namely Bartın and Zonguldak, was possible. Tables 1–3 show the locations of K-bentonite samples, mineralogical characteristics and their whole-rock major, trace and rare earth element concentrations, respectively.

Because the environmental conditions prevailing during the deposition of tephra and subsequent alteration processes reflect an open geological environment, the major-element concentrations of the whole-rock ash-fall samples (parent material of K-bentonites) are expected to change. Thus, there is a tendency to consider that the major elements do not represent the original parental source-rock compositions. Saylor *et al.* (2005) studied major element and *REE* abundances of silicified volcanic ash beds from Namibia and concluded that the whole-rock abundances of Al, Fe, Mg, K and Ti vary inversely with Si, reflecting variations in phenocryst concentration due to air fall and hydrodynamic sorting. These sorting processes did not fractionate whole-rock *REE* to a large extent; these vary more widely with Si. The *REE* abundance was independent of the position in the bed, the phenocryst abundance, or grain size, providing a geochemical means for discriminating between different ash beds. Saylor *et al.* (2005) found that the variations in the position of chondrite-normalized whole-rock *REE* plots also supported long-distance correlations of ash beds between widely separated locations. Because of the sensitivity and possible mobility of major elements to alteration processes taking place during surface weathering, burial diagenesis and low-grade metamorphism, they were not considered for geochemical fingerprinting of K-bentonites, in the present study. However, the abundances of some major elemental oxides such as CaO and MgO for samples from the Bartın area (mean values being 10.59 and 4.75%, respectively) are greater than those for the Şapca and Gökgöl K-bentonites (mean values being 5.70 and 3.35%, respectively). Higher values of Mg concentration in the Bartın-area samples may indicate either more mafic composition of the parent volcanic ash or the circulation of saline waters within the carbonate sequence enclosing the K-bentonite layers. Similarly, Fe_2O_3 abundances of Bartın samples (mean value, 4.16%) are slightly higher than those from the Şapca and Gökgöl K-bentonites (mean value, 3.53%). In contrast, the SiO_2, Al_2O_3 and K_2O percentages are comparable for all samples.

https://doi.org/10.1180/claymin.2016.051.4.02 Published online by Cambridge University Press

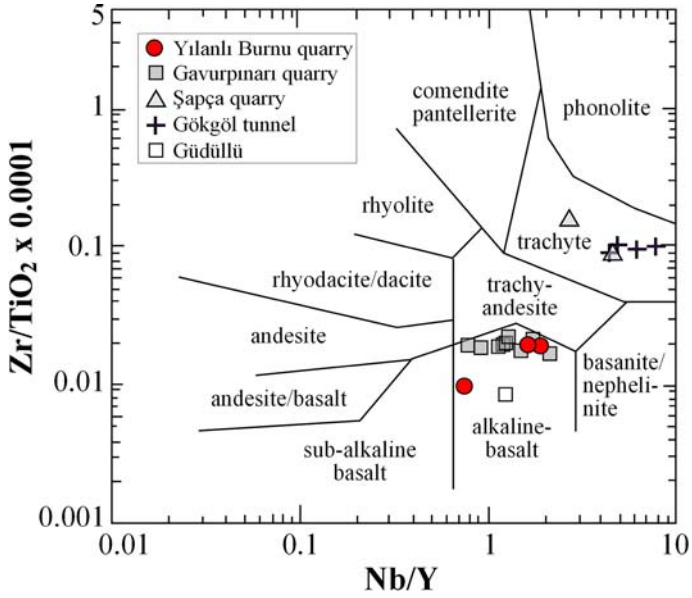

FIG. 10. Distribution of K-bentonite samples on the Zr/TiO_2-Nb/Y diagram after Winchester & Floyd (1977).

A plot based on immobile element ratios of Zr/TiO_2 *vs*. Nb/Y (Fig. 10) after Winchester & Floyd (1977) shows that K-bentonites are alkaline in nature and derived from magmas having mafic and intermediate compositions corresponding to alkali basalt and trachyte. The plot also indicates that the original compositions of the Bartın and Güdüllü samples have alkali basalt composition, whereas the Gökgöl and Şapca K-bentonites from the Zonguldak area were derived from trachytic magmas. This geochemical grouping correlates with the stratigraphic and biostratigraphic data obtained from the limestone layers adjacent to the K-bentonite beds. The foraminifera fossil record from limestone samples suggests a Late Devonian age for the Bartın and Güdüllü samples, in contrast to the Devonian–Carboniferous transition age which is assigned to samples from the Gökgöl and Şapca areas. The data suggest that the K-bentonites studied were evolved from tephras having different ages and geochemical compositions.

N-MORB-normalized trace-element data (Fig. 11a,b) confirm the similarities between the compositions of source magmas as shown in Fig. 8. The Şapca and Gökgöl K-bentonites (Fig. 11a) are characterized by positive Th and U anomalies in contrast to the negative anomalies shown by Ba and Sr. The curves from both areas match. The same graph (Fig. 11b) was used for new and previous samples from the Bartın and Güdüllü areas. As a group they exhibit the same characteristics but differ in detail from the pattern of the Şapça-Gökgöl samples.

The *REE* distribution data are shown as chondrite-normalized plots for all K-bentonites (Fig. 12). All samples have negatively sloping curves and exhibit an enrichment of light rare earth elements (*LREE*). Similar to the previous geochemical plots, the samples from Bartın and Güdüllü have similar curves and cluster in the same area in Fig. 11. The samples from the Şapca and Gökgöl locations behave as another distinct group. Both groups of samples have almost the same *LREE* slope but the heavy *REE* (*HREE*) of the Şapca samples exhibit enrichment. The presence of a negative Eu anomaly in all samples indicates fractional crystallization of plagioclase in the magmatic source rocks (*e.g.* Condie, 1978) but this fractionation is in a more advanced stage for the Şapca and Gökgöl samples having trachytic source-rock composition. The normalized *REE* plots of K-bentonite samples further suggest an interpretation concerning a tectonomagmatic origin of K-bentonites (Fig. 12). The plots of samples from the Bartın and Güdüllü groups exhibit a characteristic pattern resembling those for rocks which originated by partial melting of an

https://doi.org/10.1180/claymin.2016.051.4.02 Published online by Cambridge University Press

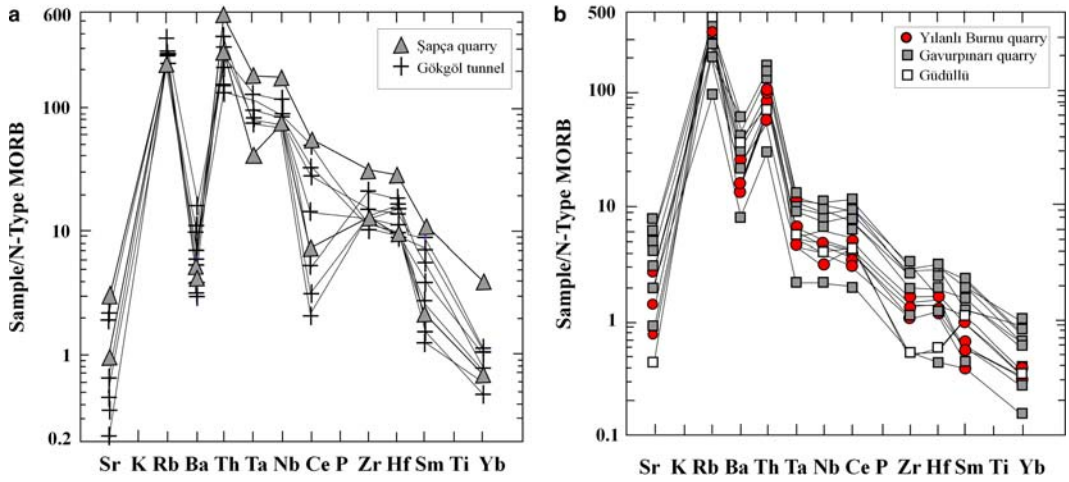

FIG. 11. N-MORB-normalized trace-element diagram (Pearce, 1974) of K-bentonites from the: (a) Şapca and Gökgöl areas; (b) Yılanlı Burnu, Gavurpınarı and Güdüllü areas.

enriched mantle (McKenzie & O'Nions, 1991). A possible site for such evolution is is a continental crustal environment affected by back-arc extension. On the other hand, plots for the other group of samples representing the Şapca and Gökgöl areas show a more distinctive Eu anomaly and enrichment of *LREE* by ~900 times compared to the chondrite. This characteristic feature relates them to alkaline rocks with a within-plate rift-related origin, as is also supported by the geochemical discrimination diagrams used for identification of tectonomagmatic setting of K-bentonites (Fig. 13a,b).

Trace-element values of SiO_2-rich samples were projected on the Rb-Y+Nb tectonic discrimination

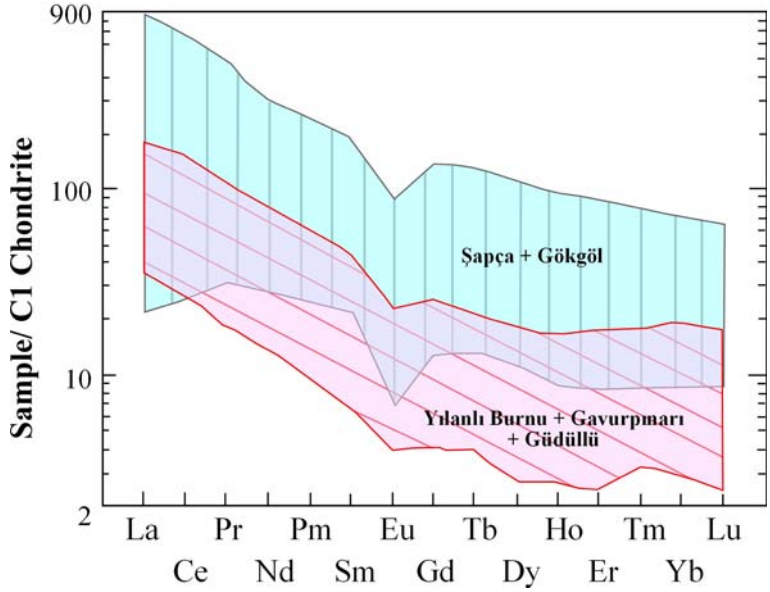

FIG. 12. Chondrite-normalized *REE* diagram (Nakamura, 1974) of K-bentonite samples from the Şapca-Gökgöl and Yılanlı Burnu-Gavurpınarı-Güdüllü areas.

https://doi.org/10.1180/claymin.2016.051.4.02 Published online by Cambridge University Press

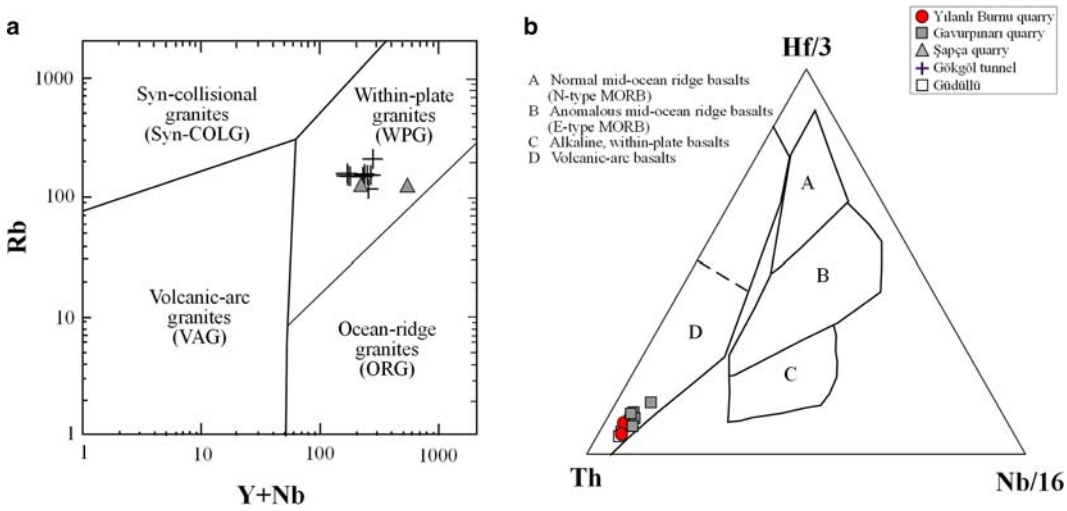

FIG. 13. (a) Distribution of K-bentonite samples from the Şapca and Gökgöl areas on the Rb-Y+Nb discrimination diagram (of Pearce *et al.,* 1984). (b) Distribution of K-bentonite samples from the Yılanlı Burnu, Gavurpınarı and Güdüllü areas on a Th-Hf-Nb discrimination diagram (Wood, 1980).

diagram (Fig. 13a) of Pearce *et al.* (1984). The geochemical signature of the Şapca and Gökgöl group which represents K-bentonite beds near the Devonian–Carboniferous boundary indicate a 'within plate' origin of trachytic source volcanism. As the alkali basalt samples from the Bartın and Güdüllü group have ocean island basalt characteristics (Fig. 12), they were not evaluated using the Rb-Y+Nb diagram (Pearce *et al.*, 1984) but by means of the Zr-Nb-Y discrimination diagram instead (Meschede, 1986), where they plot on the 'within-plate alkali basalt' field (not shown). However, when plotted on theTh-Hf-Nb (Wood, 1980) discrimination diagram (Fig. 13b), which provides a better discrimination for enriched sources, the Bartın and Güdüllü group samples plot in the calc-alkaline field indicating a subduction-modified enriched mantle source, which occurs mainly in a continental back-arc-type tectonic setting.

CONCLUSIONS

(1) New occurrences of thin K-bentonite beds in the Late Devonian–Early Carboniferous Yılanlı Formation were discovered in the Zonguldak area at the Şapca, Güdüllü and Gökgöl tunnel locations. Fossil assemblages and carbonate lithofacies types in adjacent carbonate sequences indicate that the precursor tephras were deposited in a shallow (epeiric) carbonate platform environment with tidal influence. The presence of dolostone facies indicates diagenesis in the depositional environment of the tephra layers. Accumulation of ostracods and bivalve fossils below the bentonite horizons implies that these species died *en masse* due to changes in their living conditions after deposition of the volcanic ashes.

(2) Crystal-chemical data indicate high-grade diagenesis of illites in the Bartın area and low-grade diagenesis of I-S in the Zonguldak area. Differences in the degree of illitization exist in the K-bentonite samples from three different locations in the Zonguldak area as K-bentonites from the Çukuören village area evolved more towards the illite-dominant compositions compared to samples collected at Şapca and the Gökgöl tunnel section, which belong to the illite-smectite-rich series. This interesting issue will be evaluated in detail in another study (Bozkaya *et al.*, 2016).

(3) Geochemical diagrams based on trace-element and *REE* analysis enabled the discrimination of two different groups of K-bentonites with respect to their original ash compositions. The first group consists of the Bartın and Güdüllü (Çukurören village) samples with alkali-basalt composition, whereas the second group contains Gökgöl and Şapca K-bentonites with trachytic affinities from the Zonguldak area. This geochemical grouping is in accord with the stratigraphic and biostratigraphic data obtained from the limestone layers adjacent to the K-bentonite beds.

(4) The source of the alkali basalt K-bentonites might be related to volcanism in a continental back-arc setting, which yielded the trachytic K-bentonites of the

https://doi.org/10.1180/claymin.2016.051.4.02 Published online by Cambridge University Press

second group by within-plate continental rifting. The K-bentonites from two groups of locations with different tectonomagmatic settings also have different ages, as was supported by the foraminifer fossil fauna. The first group, consisting of alkali basalt K-bentonites from the Bartın and Güdüllü locations, are Late Devonian (Late Frasnian-Famennian) in age, as opposed to the younger, trachyitic K-bentonites from the Şapca and Gökgöl locations corresponding to the Devonian–Carboniferous boundary.

(5) The source of the volcanism generating the K-bentonite beds seems to be related to large-scale volcanic eruptions during the Late Devonian and Late Devonian–Carboniferous times, whereby intensive igneous activity was in progress relating to the late Variscan closure of small Palaeozoic oceans in Laurussia (*e.g.* Günal-Türkmenoğlu, 2014). Further geochemical and biostratigraphic research is necessary to interpret the precise location of the source region.

ACKNOWLEDGEMENTS

The research described above was funded by TÜBİTAK–The Scientific and Technological Research Council of Turkey (Scientific Research Project Grant No. 110Y272). The authors thank to Prof. George E. Christidis for his editorial contributions, and Prof. Warren D. Huff and an anonymous referee for contructive comments and suggestions on the manuscript.

REFERENCES

Akbaş B, Altun I.E. & Aksay A. (2002) *1:100.000 Scaled Geological Maps. Sheet Zonguldak E28.* General Directorate of Mineral Research Exploration, Ankara, Turkey.

Algeo T.J., Berner R.A., Maynard J.P. & Scheckler S.E. (1995) Late Devonian oceanic anoxic events and biotic crises: 'Rooted' in the evolution of vascular land plants? *GSA Today*, **5**, 64–66.

Alişan C. & Derman A.S. (1995) The first palynological age, sedimentological and stratigraphic data for the Çakraz Group (Triassic), western Black Sea. Pp. 93–98 in: *Geology of The Black Sea Region: Proceedings of the International Symposium on the Geology of Black Sea Region* (A. Erler, editor). General Directorate of Mineral Research and Exploration, Ankara, Turkey.

Árkai P., Mählmann R.F., Suchý V., Balogh K., Sýkorová I. & Frey M. (2002) Possible effects of tectonic shear on phyllosilicates: a case study from the Kandersteg area, Helvetic domain, Central Alps, Switzerland. *Schweizerische Mineralogische und Petrographische Mitteilungen*, **82**, 273–290.

Aydın M., Serdar H.S., Şahintürk O., Yazman M., Çokuğraş R., Demir O. & Özcelik Y. (1987) Çamdağ (Sakarya)-Sünnicedağ (Bolu) yöresinin jeolojisi. *Bulletin of the Geological Society of Turkey*, **30**, 1–4 (in Turkish).

Bailey S.W. (1988) X-ray diffraction identification of the polytypes of mica, serpentine, and chlorite. *Clays and Clay Minerals*, **36**, 193–213.

Bergström S.M., Huff W.D., Kolata D.R. & Bauert H. (1995) Nomenclature, stratigraphy, chemical fingerprinting, and areal distribution of some Middle Ordovician K-bentonites in Baltoscandia. *Geoliska Förenigensi Stockholm Förhandingar*, **117**, 1–13.

Bozkaya Ö., Yalçın H. & Göncüoğlu M.C. (2012) Mineralogic evidences of a mid-Paleozoic tectonothermal event in the Zonguldak terrane, NW Turkey: implications for the dynamics of some Gondwana-derived terranes during the closure of the Rheic Ocean. *Canadian Journal of Earth Sciences*, **49**, 559–575.

Bozkaya Ö., Türkmenoğlu-Günal A., Göncüoğlu M.C., Ünlüce-Yücel Ö., Yılmaz I.Ö. & Schroeder P.A. (2016) Illitization of Late Devonian–Early Carboniferous K-bentonites from Western Pontides, NW Turkey: Implications for their origin and age. *Applied Clay Science*, dx.doi.org/10.1016/j.clay.2016.08.020.

Brown G. & Brindley G.W. (1980) X-ray diffraction procedures for clay mineral identification. Pp. 305–360 in: *Crystal Structures of Clay Minerals and their X-Ray Identifiction* (G. Brown & G.W. Brindley, editors). Mineralogical Society, London, UK.

Christidis G., Scott P.W. & Marcopoulos T. (1995) Origin of bentonite deposits of eastern Milos, Aegean, Greece: geological, mineralogical and geochemical evidence. *Clays and Clay Minerals*, **43**, 63–77.

Condie K.C. (1978) Geochemistry of Proterozoic granitic plutons from New Mexico, U.S.A. *Chemical Geology*, **21**, 131–149.

Dean W.T., Martin F., Monod O., Demir O., Richards R.B., Bultynck P. & Bozdoğan N. (1997) Lower Paleozoic stratigraphy, Karadere-Zirze area, Central Pontides, N Turkey. Pp. 32–38 in: *Early Paleozoic Evolution in NW Gondwana* (M.C. Göncüoğlu & A.S. Derman, editors). Turkish Association of Petroleum Geologists Special Publication, 3 pp.

Dellisanti F., Pini G.A., Tatoe F. & Bandin F. (2008) The role of tectonic shear strain on the illitization mechanism of mixed-layer illite-smectite. A case study from a fault zone in the northern Apennines, Italy. *International Journal of Earth Sciences (Geologische Rundschau)*, **97**, 601–616.

Derman A.S. (1997) Sedimentary characteristics of Early Paleozoic rocks in the western Black Sea region, Turkey. Pp. 24–31 in: *Early Paleozoic Evolution in NW Gondwana* (M.C. Göncüoğlu & A.S. Derman, editors). Turkish Association of Petroleum Geologists Special Publication, 3 pp.

Dil N. (1976) Assemblages caracteristiques de foraminiferes du Devonien superieur et du Dinantien de Turquie (Bassin Carbonifere de Zonguldak). *Annales de la Societe Geologique de Belgique*, **99**, 373–400 (in French).

Floyd P.A. & Winchester J.A. (1978) Identification and discrimination of altered and metamorphosed volcanic rocks using immobile elements. *Chemical Geology*, **21**, 291–306.

Fortey N.J., Merriman R.J. & Huff W.D. (1996) Silurian and Late-Ordovician K-bentonites as a record of late Caledonian volcanism in the British Isles. *Transactions Royal Society Edinburgh Earth Sciences*, **86**, 167–180.

Frey M. (1987) Very low-grade metamorphism of clastic sedimentary rocks. Pp. 9–58 in: *Low-Grade Metamorphism* (M. Frey, editor). Blackie, Glasgow, UK.

Gedik İ., Pehlivan S., Duru M. & Timur E. (2005) *1:50.000 Scaled Geological Maps and Explanations: Sheets Bursa G22a and İstanbul F22d.* General Directorate of Mineral Research Exploration, Ankara, Turkey.

Göncüoğlu M.C. & Kozlu H. (2000) Early Paleozoic evolution of NW Gondwanaland: data from southern Turkey and surrounding regions. *Gondwana Research*, **3**, 315–324.

Göncüoğlu M.C., Dirik K. & Kozlu H. (1997) General characteristics of pre-Alpine and Alpine terranes in Turkey: Explanatory notes to the terrane map of Turkey. *Annales Géologiques des Pays Helléniques*, **37**, 515–536.

Göncüoğlu M.C., Okuyucu C. & Dimitrova T. (2011) Late Permian (Tatarian) deposits in NW Anatolia: palaeogeographical implications. *Geoecomarina*, **17**, 79–82.

Göncüoğlu M.C., Sachanski V., Gutierrez-Marco J.C. & Okuyucu C. (2014) Ordovician graptolites from the basal part of the Palaeozoic transgressive sequence in the Karadere area, Zonguldak Terrane, NW Turkey. *Estonian Journal of Earth Sciences*, **63**, 227–232.

Grathoff G.H. & Moore D.M. (1996) Illite polytype quantification using Wildfire©-calculated X-ray diffraction patterns. *Clays and Clay Minerals*, **44**, 835–842.

Guggenheim S., Bain D.C., Bergaya F., Brigatti M.F., Drits V., Eberl D.D., Formoso M., Galán E., Merriman R.J. & Peacor D.R. (2002) Report of the Association Internationale pour L'etude des Argiles (AIPEA) Nomenclature Committee for 2001: Order, disorder, and crystallinity in phyllosilicates and the use of the 'crystallinity' index. *Clay Minerals*, **37**, 389–393.

Guidotti C.V., Mazzoli C., Sassi F.P. & Blencoe J.G. (1992) Compositional controls on the cell dimensions of 2M1 muscovite and paragonite. *European Journal of Mineralogy*, **4**, 283–297.

Günal Türkmenoğlu A., Bozkaya Ö., Ünlüce Yücel Ö., Göncüoğlu M.C. & Yılmaz İ.Ö. (2012) Zonguldak-Bartın (Batı Karadeniz) bölgesindeki Devoniyen yaşlı K-bentonitlerin kil mineralojisi. *15th National Clay Symposium, Proceedings*, 29–42, Niğde, Turkey (in Turkish).

Günal Türkmenoğlu A., Bozkaya Ö., Göncüoğlu M.C., Ünlüce Yücel Ö., Yılmaz İ.Ö. & Okuyucu C. (2015) Clay mineralogy, chemistry, and diagenesis of Late Devonian K-bentonite occurrences in northwestern Turkey. *Turkish Journal of Earth Sciences*, **24**, 209–229.

Histon K., Klein P., Schönlaub H.P. & Huff W.D. (2007) Lower Paleozoic K-bentonites from Carnic Alps, Austria. *Austrian Journal of Earth Sciences*, **100**, 26–42.

Hoffman J. & Hower J. (1979) Clay mineral assemblages as low grade metamorphic geothermometers: application to the thrust faulted disturbed belt of Montana, U.S.A. Pp. 55–79 in: *Aspects of Diagenesis* (P.A. Scholle & R. Schluger, editors). SEPM Special Publication, **26**, Society for Sedimentary Geology, Tulsa, Oklahoma, USA.

Huff W.D. & Morgan D.J. (1990) Stratigraphy, mineralogy and tectonic setting of Silurian K-bentonites in southern England and Wales. *9th International Clay Conference*, 33–42, Strasbourg, France.

Huff W.D. & Türkmenoğlu A.G. (1981) Chemical characteristics and origin of Ordovician K-bentonites along the Cincinnati Arch. *Clays and Clay Minerals*, **29**, 113–123.

Huff W.D., Bergström S.M. & Kolata D.R. (1992) Gigantic Ordovician ash fall in North America and Europe: Biological, tectonomagmatic and event-stratigraphic significance. *Geology*, **20**, 875–878.

Huff W.D., Bergström S.M., Kolata D.R. & Sun H. (1997) The Lower Silurian Osmundsberg K-bentonite. Part II: mineralogy, geochemistry, chemostratigraphy and tectonomagmatic significance. *Geological Magazine*, **135**, 15–26.

Izett G.A. (1981) Volcanic ash beds: Recorders of Upper Cenozoic silisic pyroclastic volcanism in the western United States. *Journal of Geophysical Research*, **86**, 10200–10222.

Jackson M.L. (1969) *Soil Chemical Analysis: Advanced Course* (2nd edition). Published by the author, Department of Soil Science, Univeristy of Wisconsin, Madison, Wisconsin, USA.

Kalvoda J. (2001) Upper Devonian–Upper Carboniferous foraminiferal paleobiogeography and Perigondwana terranes at the Baltica-Gondwana interface. *Geologica Carpathica*, **52**, 205–215.

Kerey I.E. (1984) Facies and tectonic setting of the upper Carboniferous rocks of NW Turkey. Pp. 123–128 in: *The Geological Evolution of the Eastern Mediterranean* (A.H.F. Robertson & J. Dixon, editors). Blackwell Scientific, Oxford, UK.

Kisch H.J. (1991) Illite crystallinity: recommendations on sample preparation X-ray diffraction settings and inter-

laboratory samples. *Journal of Metamorphic Geology*, **9**, 665–670.

Kolata D.R., Frost J.K. & Huff W.D. (1987) Chemical correlation of K-bentonites in the Middle Ordovician Decorah Subgroup, upper Mississippi Valley. *Geology*, **15**, 208–211.

Kolata D.R., Huff W.D. & Bergström S.M. (1998) Nature and regional significance of unconformities associated with the Middle Ordovician Hagan K-bentonite complex in the North American midcontinent. *Geological Society of American Bulletin*, **110**, 723–739.

Kübler B. (1968) Evaluation quantitative du metamorphisme par la cristallinite de l'illite. *Bulletin-Centre de Recherches Pau-SNPA*, **2**, 385–397.

Mamet B.L. & Preat A. (2009) Middle Devonian algal and problematic microfossils of the 'Frondry des Chiens' (southern border of Dinant Synclinorium, Belgium): Paleobathymetric implications. *Revue de Micropaleontologia*, **52**, 249–263.

McKenzie D. & O'Nions R.K. (1991) Partial melt distributions from inversion of rare earth element concentrations. *Journal of Petrology*, **32**, 1021–1091.

Merriman R.J. & Frey M. (1999) Patterns of very low-grade metamorphism in metapelitic rocks. Pp. 61–107 in: *Low-Grade Metamorphism* (M. Frey & D. Robinson, editors). Blackwell Science, Oxford, UK.

Merriman R.J. & Peacor D.R. (1999) Very low-grade metapelites: mineralogy, microfabrics and measuring reaction progress. Pp. 10–60 in: *Low-Grade Metamorphism* (M. Frey & D. Robinson, editors). Blackwell Science, Oxford, UK.

Merriman R.J. & Roberts B. (1990) Metabentonites in the Moffat shale Group, Southern uplands of Scotland: Geochemical evidence of ensialic marginal basin volcanism. *Geological Magazine*, **127**, 259–271.

Meschede M. (1986) A method of discriminating between different types of mid-ocean ridge basalts and continental tholeiites with the Nb-Zr-Y diagram. *Chemical Geology*, **56**, 207–218.

Min K., Renne P.R. & Huff W.D. (2001) $^{40}Ar/^{39}Ar$ dating of Ordovician K-bentonites in Laurentia and Baltoscandia. *Earth and Planetary Science Letters*, **185**, 121–134.

Moore D.M. & Reynolds R.C. Jr (1997) *X-ray Diffraction and the Identification and Analysis of Clay Minerals* 2nd edition. Oxford University Press, New York.

Nakamura N. (1974) Determination of REE, Ba, Fe, Mg, Na and K in carbonaceous and ordinary chondrites. *Geochimica et Cosmochimica Acta*, **38**, 757–775.

Özkan R. & Vachard D. (2015) A new early Frasnian (Late Devonian) foraminifer from eastern Taurides (Turkey): Evolutionary and paleobiogeographic implications. *Revue de Micropaleontologie*, **58**, 267–282.

Pearce J.A. (1974) Statistical analysis of major element patterns in basalts. *Journal of Petrology*, **17**, 15–43.

Pearce C.A., Harris N.B.W. & Tindle A.G. (1984) Trace element discrimation diagrams for the tectonic interpretation of granitic rocks. *Journal of Petrology*, **25**, 956–983.

Poyarkov B.V. (1969) Stratigraphy and foraminifers of the Devonian system in the Tian-Shian (in Russian). *Akad. Nauk Kirgiz. SSR, Inst. Geol., Izdatel. Ilim, Frounze*, 1–186.

Racki G. & Sobon-Podgorska J. (1993) Givetian and Frasnian calcareous microbiatas of the Holy Cross Mountains. *Acta Palaentologica Polonica*, **37**, 255–289.

Sabirov A.A. (2004) Pre-Visean foraminifers from Central Asia and Kazakhstan. *Paleontological Journal*, **38**, 238–246.

Schanski V., Göncüoğlu M.C. & Gedik I. (2010) Late Telychian (Early Silurian) graptolitic shales and the maximum Silurian highstand in the NW Anatolian Palaeozoic terranes. *Palaeogeography, Palaeoclimatology, Palaeoecology*, **291**, 419–428.

Saylor B.Z., Poling J.M. & Huff W.D. (2005) Stratigraphic and chemical correlation of volcanic ash beds in the terminal Proterozoic Nama Group, Namibia. *Geological Magazine*, **142**, 519–538.

Taylor S.R. & McLennan S.M. (1988) The significance of rare earths in geochemistry and cosmochemistry. Pp. 485–578 in: *Handbook on Physics and Chemistry of Rare Earths* (K.A. Gschneider & L. Eyring, editors). Elsevier, New York.

Teale C.T. & Spears D.A. (1986) The mineralogy and origin of some Silurian bentonites, Welsh Borderland, U.K. *Sedimentology*, **33**, 757–65.

Türkmenoğlu A. (2001) A Paleozoic K-bentonite occurrence in Turkey. In: *Mid-European Clay Conference'01*. Book of Abstracts, Stara Leusa, Slovakia.

Türkmenoğlu A., Göncüoğlu M.C. & Bayraktaroğlu Ş. (2009) Early Carboniferous K-bentonite formation around Bartın: Geological implications. Pp. 209 in: *2nd International Symposium on the Geology of the Black Sea Region*, İstanbul, Turkey.

Vachard D. (1991) Parathuramminides et Moravamminides (Microproblematica) de l'emsien superieur de la formation Moniello (Cordilleres Cantabriques, Espagne). *Revue de Paléobiologie*, **10**, 255–299.

Vachard D. (1994) Foraminiferes et Moravamminides du domaine Ligerien (Massif Armoricain, France). *Palaeontographica Abteilung A-Paläozoologie-Stratigraphie*, **A 231**, 1–92.

Vachard D., Zahraoui M. & Cattaneo G. (1994) Parathuramminines et Moravamminides (Foraminiferes?) du Givetien du Maroc Central. *Revue de Paléobiologie*, **14**, 1–19.

Ver Straeten C.A. (2004) K-bentonites, volcanic ash preservation, and implications for Early to Middle Devonian volcanism in the Acadian orogen, eastern North America. *Geological Society of America Bulletin*, **116**, 474–489.

Vissarionova A.Ya. (1950) Faune de foraminiféres du Dévonien de Bachkirie. *Bachkir*, **1**, 34–37.

https://doi.org/10.1180/claymin.2016.051.4.02 Published online by Cambridge University Press

Warr L.N. & Ferreiro Mahlmann R. (2015) Recommendations for Kübler Index standardization. *Clay Minerals*, **50**, 283–286.

Warr L.N. & Rice A.H.N. (1994) Interlaboratory standardisation and calibration of clay mineral crystallinity and crystallite size data. *Journal of Metamorphic Geology*, **12**, 141–152.

Weaver C.E. (1953) Mineralogy and Petrology of some Ordovician K-bentonites and related linestones. *Geological Society of America Bulletin*, **64**, 921–944.

Winchester J.A. & Floyd P.A. (1977) Geochemical discrimination of different magma series and their differentiation products using immobile elements. *Chemical Geology*, **20**, 325–343.

Wood D.A. (1980) The application of a Th-Hf-Ta diagram to problems of tectonomagmatic classification and to establishing the nature of crustal contamination of basaltic lavas of the British Tertiary volcanic province. *Earth and Planetary Science Letters*, **50**, 11–30.

Yalçın M.N. & Yılmaz I. (2010) Devonian in Turkey – a review. *Geologica Carpathica*, **61**, 235–253.

Yanev S., Göncüoğlu M.C., Gedik I., Lakova I., Boncheva I., Sachanski V., Okuyucu C., Özgül N., Timur E. & Maliakov Y. (2006) Stratigraphy, correlations and palaeogeography of Palaeozoic terranes of Bulgaria and NW Turkey: a review of recent data. Pp. 51–67 in: *Tectonic Development of the Eastern Mediterranean Region* (A.H.F. Robertson & D. Mountrakis, editors). Special Publications **260**, Geological Society of London, UK, 260 pp.

https://doi.org/10.1180/claymin.2016.051.4.02 Published online by Cambridge University Press